Charles University

Faculty of Science

Study programme: Biology

Branch of study: Cellular and Developmental Biology

Bc. Tereza Bělinová

Effects of silicon nanoparticles on human cells

Sledování vlivu křemíkových nanočástic na lidské buňky

Diploma thesis

Supervisor: doc. RNDr. Marie Hubálek Kalbáčová, Ph.D.

Prague, 2017

Prohlášení:

Prohlašuji, že jsem závěrečnou práci zpracovala samostatně a že jsem uvedla všechny použité informační zdroje a literaturu. Tato práce ani její podstatná část nebyla předložena k získání jiného nebo stejného akademického titulu.

V Praze, 14. 08. 2017

.....

Tereza Bělinová

Acknowledgements:

Here I would like to express my deepest gratitude to my supervisor Marie Hubálek Kalbáčová who supported me and provided me with valuable guidance through the past years. My thanks also belong to Blanka Bílková, Pavla Sauerová and Lucie Vrabcová. Without their support and help this thesis could never be completed. Also, I am very grateful for the help of other collaborators mentioned in the thesis and lab members of Institute of inherited metabolic diseases who provided me with their advices and great working environment. Last, but not least my thanks go to my family, without their support I would have never gone so far.

This study was supported by Visegrad Group (V4)-Japan Joint Research Program on Advanced Materials (project NaMSeN) and by the project of National Sustainability Program I No. LO1503

Abstract

In past years, nanoparticles have been studied as possible platform to be used in biomedicine. In order to establish the application potential of nanoparticles, its impact to biological systems have to be determined. Herein, several silicon-based nanoparticles of different origins were studied in respect of their influence on metabolic activity of human cells, namely osteoblast cell line SAOS-2 and monocytic cell line THP-1. The obtained results proposed that the impact of nanoparticles on cells is highly dependent on cultivation conditions in which nanoparticles are administered to cells. Furthermore, microscopy experiments were implemented in order to localize the particles within cells, where conventional microscopy limitations are evident.

Key words: *silicon nanoparticles, quantum dots, cell-particle interaction, cytotoxicity*

Abstrakt

V posledních několika letech byly nanočástice studovány, jako možná platforma pro využití v biomedicíně. Pro určení správného aplikačního potenciálu těchto materiálů, je nejprve nutno charakterizovat jejich vliv na biologické systémy. Bylo studováno několik typů nanočástic na bázi křemíku s ohledem na jejich vliv na metabolickou aktivitu lidských buněk, jmenovitě osteoblastové (SAOS-2) a monocytární (THP-1) linie. Získané výsledky naznačují, že vliv částic na buňky je úzce svázán s kultivačními podmínkami, ve kterých jsou částice buňkám představeny. Navíc bylo provedeno několik mikroskopických experimentů za účelem lokalizace částic v buňkách. Konvenční mikroskopické metody se ovšem v tomto případě ukázaly značně limitující.

Klíčová slova: *křemíkové nanočástice, kvantové tečky, interakce buňka-částice, cytotoxicita*

Table of contents

1. Introduction 9
2. Aims of The Work 10
3. Literature Overview 11
3.2. Nanomaterials in Biology 11
3.2.1. Nanomaterial Definition 11
3.2.2. Silicon Based Nanoparticles and Their Current Use in Biological Context 11
3.3. Particle-cell Interaction 12
3.3.1. Cellular Uptake 12
3.3.2. Biomolecular Corona and Its Roles in Particle-Cell Interaction 13
3.3.3. Specific Cellular Uptake Mechanisms of Nanoparticles 14
3.3.4. Effects of Nanoparticles on Cells 16
3.3.5. Exocytosis 18
4. Materials and Methods 21
4.1. Cell Culture 21
4.1.1. Cell Lines and Cultivation Conditions 21
4.1.2. Subculturing 21
4.1.3. Freezing and Thawing of Cells 21
4.1.4. Experimental Conditions 22
4.1.5. Doubling Time Establishment 23
4.1.6. Differentiation of THP-1 Cells 23
4.2. Particle Characterization 23
4.3. Determination of Metabolic Activity 24
4.4. Apoptosis Detection 25
4.5. Lactate Dehydrogenase Assay 25
4.6. Flow Cytometry 26
4.7. Fluorescence Staining 26

4.8. Microscopy 27
4.9. Two-Photon Excitation Microscopy 28
4.10. Electron Microscopy 28
4.11. Statistical Analysis 29
5. Results 30
5.2. Preliminary Results 30
5.2.1. Cell Characterization 30
5.2.2. Cultivation Conditions Establishment 34
5.3. Cytotoxicity Experiments 37
5.3.1. SiQD (Japan) 37
5.3.2. SiC (Hungary) 45
5.3.3. SiNP (Czech Republic) 47
5.4. Microscopy Experiments 48
5.4.1. SiQD (Japan) 49
5.4.2. SiC (Hungary) 52
5.4.3. SiNP (Czech Republic) 54
5.4.4. Transmission Electron Microscopy 56
6. Discussion 58
6.2. Preliminary Results 58
6.3. SiQD (Japan) 59
6.4. SiC (Hungary) 61
6.5. SiNP (Czech Republic) 62
6.6. Summary 63
7. Conclusions 64
8. References 66

List of abbrevations

BSA	bovine serum albumine
DAPI	4',6-diamidin-2-fenylindol
DIC	differential interference contrast/Nomarski contrast
DMEM	Dulbecco's Modified Eagle Medium
DMSO	dimethylsulfoxide
EDTA	Ethylenediaminetetraacetic acid
FBS	foetal bovine serum
FITC	fluorescein
FSC	forward scatter
HPS	human plasma serum
LDH	lactate dehydrogenase
MilliQ	ultrapure water
MTS	tetrazolium compound
NAD/NADH	Nicotinamide adenine dinucleotide
nm	nanometer
NP	nanoparticle
PBS	phospate buffer saline
PMA	Phorbol 12-myristate 13-acetate
QD	quantum dot
SiC	silicon nanoparticles - Hungarian origin
SiO2	silicone dioxide
SiQD	silicon nanoparticle - Japan origin
SSC	side scatter
TEM	transmission electron microscopy
ÚHKT	Institute of Hematology and Blood Transfusion

1. Introduction

In past decade, researches´ focus on nanoparticle-cell interaction has been growing in numbers. Nanoparticles are interesting for their application in biomedicine as possible drug and gene carriers or imaging and diagnostic platforms. Researches in this field focus not only on establishing the behaviour of nanoparticles in biological context, but also on possible cytotoxicity and its mechanism. Currently, the most commonly used nanoparticles are organic polymers, however, growing interest is being given to inorganic, yet biocompatible materials, such as silicon. The following brief literature overview shall provide the reader with insight into nanoparticle-cell interactions, and possible use of the presented findings. All of the cited works are either directly connected with nanoparticles based on silicon, or the results propose a new direction, which may be adapted to silicon nanoparticle field.

2. Aims of The Work

- Determine influence of supplementation with serum on metabolic activity of human cells
- Determine influence of SiQD on viability of human cells under different cultivation conditions
- Determine influence of SiC on viability of human cells under different cultivation conditions
- Determine influence of SiNP on viability of human cells
- Use microscopy techniques to observe different types of silicon based nanoparticles in human cells

3. Literature Overview

3.2. Nanomaterials in Biology

3.2.1. Nanomaterial Definition

Commonly used definition of nanomaterial states that the nanomaterial should possess at least one external dimension in the range from 1 to 100 nanometres (nm). Specifically, nanoparticles must possess all their outer dimensions in this range. In case that one of the outer dimensions is approximately three times bigger than the rest, a term nanofiber can be used. In addition to the previously stated, a special type of nanoparticles – so called quantum dots (QDs) – exists. These particles possess all external dimensions in the range from 1 to 10 nm and have multiple specific characteristics. ("ISO/TS 27687" 2012)

The materials used for fabrication of nanostructures varies from single element compounds (mainly metals) and different oxides to complex polymeric structures. Each of the materials used possess different advantages and disadvantages, like easy fabrication methods or the possibility of alteration of material structure in case of polymeric structures. For the use of said materials in biology or biomedicine, biological compatibility and biodegradability is crucial.

Nowadays mostly nanofibers are widely used, as to the expansion of artificial scaffolding in tissue engineering. As for nanoparticles and QDs the use is limited to various *in vitro* studies and few *in vivo* studies, which, however, showed a lot of problems in their degradation by living organisms (Li et al., 2015).

3.2.2. Silicon Based Nanoparticles and Their Current Use in Biological Context

Thanks to its high biocompatibility, biodegradability and modifying capability silicon is being given more and more attention in the field of biomedical application (Anglin et al., 2004; Halas, 2008). Silicon based nanoparticles are often porous, which provides an idea of their usage as drug delivery platform, *in vitro* and possibly *in vivo* imaging probes and biosensors (Athinarayanan et al. 2015; Peng et al., 2014; Tamba et al., 2015; Zhang et al., 2013). However, when speaking of silicon-based nanoparticles, usually the term silicon QDs arises.

Quantum dots are particles specifically made of semiconductors such as germanium or silicon, with a heavy metal core (for example cadmium). The key characteristic of QDs is their

chemical purity, photoluminescence upon excitation, high quantum yield and resistance to photobleaching (Drbohlavova et al. 2009). Mainly thanks to their optical properties, QDs are viewed as promising platform to replace currently used fluorescent dyes or to be used as effective biosensors (Shao et al. 2011). However, most of the commonly used QDs are based on heavy metals and other not fully biocompatible materials, which proves to be complicated. Upon contact with biological environment, the coating, which is usually bound to QDs is processed and the harmful core is released causing significant cytotoxicity (Han et al., 2012; Rejman et al., 2004; Zheng et al., 2011). Regarding this, current researches focus on establishing more biocompatible QDs. Silicon QDs possess the advantage of not having heavy metal core, thus shifting silicon based QDs to interest of multiple research groups.

3.3. Particle-cell Interaction

3.3.1. Cellular Uptake

There are multiple ways cell can internalize extracellular materials; each of them is specific in its function. Smaller molecules or ions can be transported through plasmatic membrane by passive diffusion or with the help of carrier proteins or ion pumps. However, when speaking of internalization of bigger structures, endocytic mechanisms are applied. Endocytic mechanisms differ in their specificity. Pinocytosis and macro-pinocytosis – which can be both translated as “cellular drinking” – are typical examples of nonspecific endocytic pathways. Pinocytosis is characterized by absorption of extracellular fluids, small molecules and vesicles not bigger than 100 nanometres. Macro-pinocytosis on the other hand can internalize and form vesicles up to 5 micrometres. Clathrin and caveolin (or sometimes flotillin) mediated endocytosis and phagocytosis are then highly specific processes. Phagocytosis is however restricted upon professional phagocytes such as macrophages or dendritic cells. Both processes are receptor-mediated, which provides certain specificity (The Cell: A Molecular Approach. 2nd edition).

Generally, endocytosis involves engulfing of extracellular material by plasmatic membrane protrusions, which fuse and form intracellular vesicle. This vesicle containing internalized material is called early endosome and some degradation processes start. These processes slowly shift intra-vesicular pH from 6.5 in early endosome to pH 5 – 6. This more acidic pH defies so called late endosome, which is capable of fusing with vesicles from Golgi

apparatus forming a lysosome, where path of most macromolecules ends by proteasomal degradation in pH around 4.

3.3.2. Biomolecular Corona and Its Roles in Particle-Cell Interaction

The particle-cell interaction *in vitro* is mediated via cultivation media and *in vivo* by biological fluids (blood, etc.). Of course, nanoparticles may be experimentally internalized into cells directly using for example electroporation or microfluidics, however, these approaches on purpose skip the physiological interaction. Cultivation media or biological fluids contain various types of biomolecules, such as sugars and proteins, and these molecules tend to bind to the surface of particle forming so called biomolecular corona (fig. 1). This corona is basically a layer of biomolecules attached to particles using weak electrochemical interactions and is based on particle surface properties (Gagner et al., 2012; Monopoli et al., 2012).

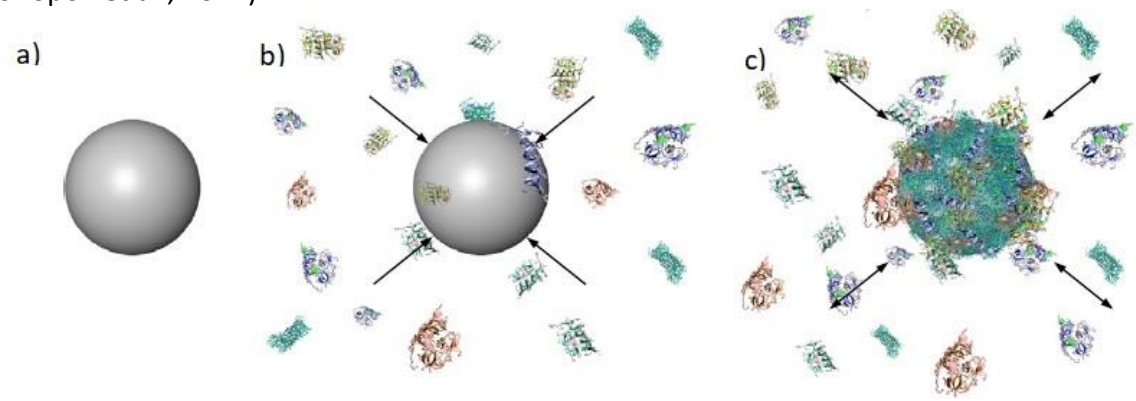

Figure 1: Schematic representation of formation of biomolecular corona. a) bare particle, b) formation of "hard" corona, c) formation of dynamic "soft" corona (Elsaesser & Howard, 2012)

It is commonly accepted that the biomolecular corona itself has two layers. First layer of so called "hard" corona (directly bound to particle surface) and second layer, "soft" corona. These layers differ in their stability. The "hard" corona is typically formed within few seconds after contact with biological environment and stays stable in time. The "soft" corona on the other hand is not bound to the nanoparticle surface strongly and changes in time (Casals & Puntes, 2012). The formation of the biomolecular corona seems to be highly important as some researches showed significant decrease of cellular viability when nearly no corona was present (Lesniak et al., 2012; Ostrovska et al., 2016; Tenzer et al., 2013). The absence of corona may be achieved by removing foetal bovine serum from cultivation media, which takes away the molecules that normally form the corona (Lesniak et al., 2012).

Deeper studies of this phenomenon could provide us with valuable information for future use of particular nanoparticles.

One can say that the corona defines particle identity. This identity then mediates the particle-cell interaction and deeper understanding of the way how biomolecular corona works could help us with targeting of the particles. Some studies suggest that the formation of corona takes place within several seconds after internalization, which means that the conditions at the time of administration and shortly after are crucial for future fate of the particle (Tenzer et al., 2013). The exact composition of the corona is, however, hard to precisely predict. Some researches proposed that it is not given that the corona will be composed of the molecules with the biggest electrochemical affinity to the particle (Monopoli et al., 2012). Fabrication of nanoparticles with specifically modified surface in order to direct them into specific cells or organelles seems to be an interesting option for targeted drug delivery. However, the formation of corona is capable of hiding these modifications, which lessens their meaning (Salvati et al., 2013). Recently, precoating of nanoparticle by targeting proteins has been proposed and is seemingly the path to follow when trying to systematically target the particles to specific cells or tissues (Mirshafiee et al., 2016). This hunt to discover precise mechanism of corona formation and subsequently possibilities for nanoparticles targeting is driven by the desire to form nanoparticle based drug carrier to selectively deliver medications to desired tissue. This targeting is promising for example to avoid systemic influence of cancer treatments and to focus only on affected cells. However, Salvati et al. proposed that the issue of targeting is extremely complex and depends on multiple factors that are not easily managed (Salvati et al., 2013).

The impact of biomolecular corona is not only in defying cellular identity but also in defying the changes in nanoparticle affinition caused by proteins coating, which may lead to formation of clusters (Moerz et al., 2015). The clusters possess different size and shape than the bare and single particles and it may have a huge impact on cellular uptake and further fate within the cell.

3.3.3. Specific Cellular Uptake Mechanisms of Nanoparticles

Significant number of researches proved, that nanoparticles are internalized into cells by active mechanisms (fig. 2). This was proven by blocking of ATP production (active

processes) by incubation of cells with nanoparticles at 4°C (Herd et al., 2013; Perevedentseva et al., 2013).

A significant number of researches has focused on the discovery of exact endocytic pathways involved in nanoparticle uptake. It is probable that when particles occur in biological environment in high enough concentration, they will eventually enter the cell in non-specific way. This, however, is not desirable for further research purposes and thus researchers try to figure out specific ways of nanoparticles usage.

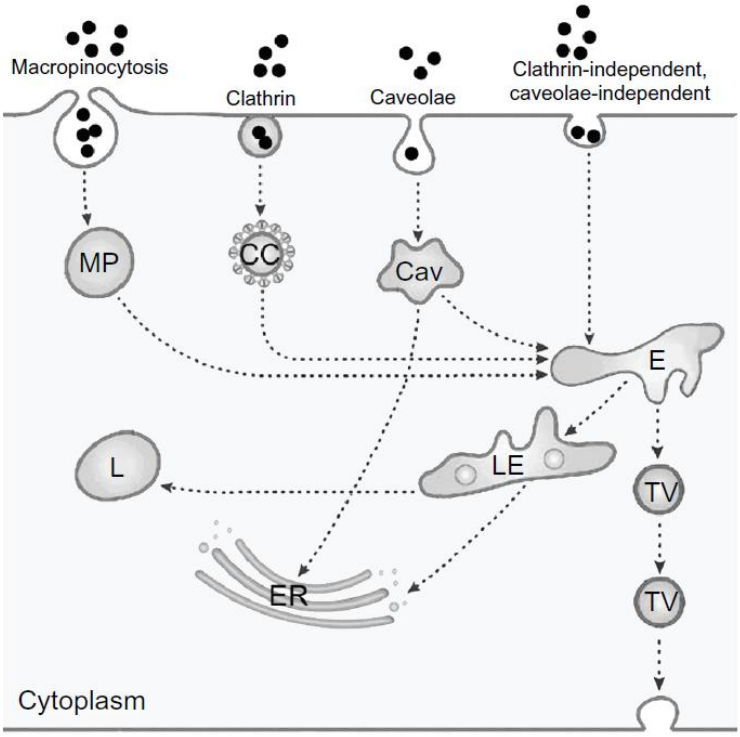

Figure 2.: Schematic representation of different ways nanoparticles are internalized into cells (MP – macropinosome, CC – clathrin coated vesicle, Cav – caveosome, E – early endosome, LE – late endosome, TV – trans vesicle, L – lysosome, ER – endoplasmic reticule) (Fröhlich 2012)

It has been long proven that particle shape, size and surface chemistry are defying variables that affects endocytic mechanism of their uptake (Gratton et al., 2008; Jiang et al., 2008; Slowing et al.,2006; Trewyn et al., 2008). Usually the uptake mechanisms are studied by selective blocking of one of them. For example, Kuhn et al. used specific inhibitors to identify internalization way of polystyrene particles. They proposed that macrophages are capable of internalization of particles in multiple ways (phagocytosis, macro-pinocytosis and clathrin-dependent endocytosis) and also reported that particle size is one of the most crucial parameters involved in endocytosis of particles (Kuhn et al., 2014). Another collective

of authors has tested different shapes of silica (SiO_2) based nanoparticles. Nanoparticles used in this study used clathrin-dependent endocytosis and macro-pinocytosis again. They also presented evidence of macrophages (RAW cells – immortalized mouse macrophage line) using phagocytosis to ingest nanoparticles (Herd et al., 2013). Different group showed quite similar results when testing SiO_2 nanoparticles on human alveolar epithelial cells. They convincingly proved that their nanoparticles enter the cells by actin dependent endocytosis by blocking it with cytochalasin D. They also provided some evidence that the presence of serum proteins in cultivation media, being connected with presence of biomolecular corona, decreases significantly the nanoparticle uptake (Nowak et al., 2014). Beside the previously cited results, proves of flotillin-dependent endocytosis can be also found. However, the authors themselves state that clathrin- and caveolin-independent pathways of uptake are extremely rare (Kasper et al., 2013).

The effect of molecular corona on cellular uptake of nanoparticles is being discussed broadly in many articles and studies and seems to be, beside size and shape, the key mechanism defying cellular uptake (Brownet al., 2014; Burdette et al., 2016; Kasper et al., 2013). However, Treuel et al. proposed an interesting idea that the presence or absence of corona modifies only the actual binding of dihydrolipoic acid-coated quantum dots particles to cellular membrane and not the endocytic mechanisms (Treuel et al., 2014). This idea provides space for specific cellular targeting of nanoparticles specifically by modification of proteins bound to them. The adaptation of this finding on silicon based nanoparticles would open a new field for their usage.

All of the previously cited studies worked with different types of nanoparticles of different origins and characteristic and the results, which in some cases have even been contradictory, show, that each particle is different. This means that every material and especially every nanoscale material should be studied broadly and no information cannot be taken for granted.

3.3.4. Effects of Nanoparticles on Cells

While external material absorbed by cell progresses within the endocytic pathway, the digestion may affect also internalized nanoparticles. The fate of particles within the cell is extremely hard to observe and nearly none exact data exist. However, biomolecular data can provide us with evidences of possible cytotoxicity mechanisms.

The harmfulness of particles is caused by multiple mechanisms. Of course, the material (chemistry) of nanoparticle possesses a key role, as potentially toxic materials (e.g. heavy metals) would be toxic regardless of other factors. However, currently, two main causes of toxicity are discussed the most. It is the size of nanoparticles and the presence or more precisely the absence of biomolecular corona. Other properties such as surface modifications, electrostatics or particle morphology can also play a role in toxicity, however, not so much importance is given to them so far. Beside nanoparticles' properties, the cell type has also significant impact (Kim et al., 2015; Wu et al., 2015).

The size dependent cytotoxicity of silica based nanoparticles is nicely described in early paper of Napierska et al. They used two sizes of the same nanoparticles and proved that smaller particles affect cellular viability more than bigger ones. Moreover, the mechanism of damage was slightly different. In case of smaller particles (approx. 20 nm in diameter), the first changes in cellular morphology could be observed within 1 hour since nanoparticles administration. The bigger particles (approx. 100 and 300 nm in diameter) took longer to affect the cells. The time dependence of affection can point out to the mechanism of cellular death as necrosis is a fast process and apoptosis is significantly slower (Napierska et al., 2009). Their results were a nice example of how size of nanoparticles can affect cellular viability, however, later studies showed, that the size dependence is also highly cell type specific (Kim et al., 2015).

The importance of the presence of biomolecular corona has been pointed out by several studies (Lesniak et al., 2012; Ostrovska et al., 2016; Tenzer et al., 2013). The absence of biomolecular corona is commonly simulated by incubation of cells with nanoparticles in medium without addition of foetal bovine sera as a supplement. The results then show faster and higher uptake of particles in serum free conditions. Lesniak et al. proposed that it can be caused by observed higher adhesion of "naked" nanoparticles on cellular membrane in contrast to corona engulfed nanoparticles (Lesniak et al., 2012).

The correlation between size or protein corona absence and subsequent cytotoxicity seems to be quite clear, however, the precise mechanism of toxicity itself is not understood well yet. It is due to the lack of sufficient methods to convincingly prove the exact mechanisms. Usually, cellular viability is being assessed by MTT assay (colorimetric assay reporting activity of mitochondrial reductase in cells) and the results are correlated with

either apoptosis or necrosis detection, or genotoxicity studies. However, the reason why cellular viability is lowered and why the cells tend to die is unclear.

As stated before, the causes of cytotoxicity are yet to be specified. Several researches showed reactive oxygen species (ROS) generation connected with nanoparticle endocytosis (Guo et al., 2015; Chu et al., 2012; Lehman et al., 2016). Chu et al even proposed ROS generation to be one of the reasons for apoptosis in cells, which came in contact with nanoparticles.

All researchers so far observed that silicon based nanoparticles affect cells. The cytotoxic influence can be generally observed upon high dosage of particles administered to cells and is shape and biomolecular corona dependent, as well as size and material properties dependent. It is common to use particles varying in size from approximately 10 to 200 nanometres in diameter. The particles used for this thesis are unique in respect to size as they are significantly smaller (approx. 4-6 nanometres in diameter).

3.3.5. Exocytosis

The progression through endocytic pathways may eventually end by exocytosis, which is generally an active process. Any molecule, which is internalized into cell by one of endocytic mechanisms either ends in lysosome or is only trafficked via transcytosis and leaves the cell. The decision process of further fate of the engulfed material is decided in early endosome, which sorts its cargo either to Golgi apparatus, for recycling on cellular membrane or for progression to late endosome and lysosome.

When talking about the potential use of nanoparticles in biomedicine, it is only obvious that all aspects of nanoparticle trafficking must be specified. It is surprising that not much attention is being given to the mechanisms the cells use to remove nanoparticles. Only a small amount of studies is available in this field, which might be caused by absence of well-established methods for its observation.

The mechanism of exocytosis possibly depends on the endocytic mechanisms as schematically showed in Fig. 3. The mechanism of endocytosis of nanoparticles and the influencing properties has been discussed earlier.

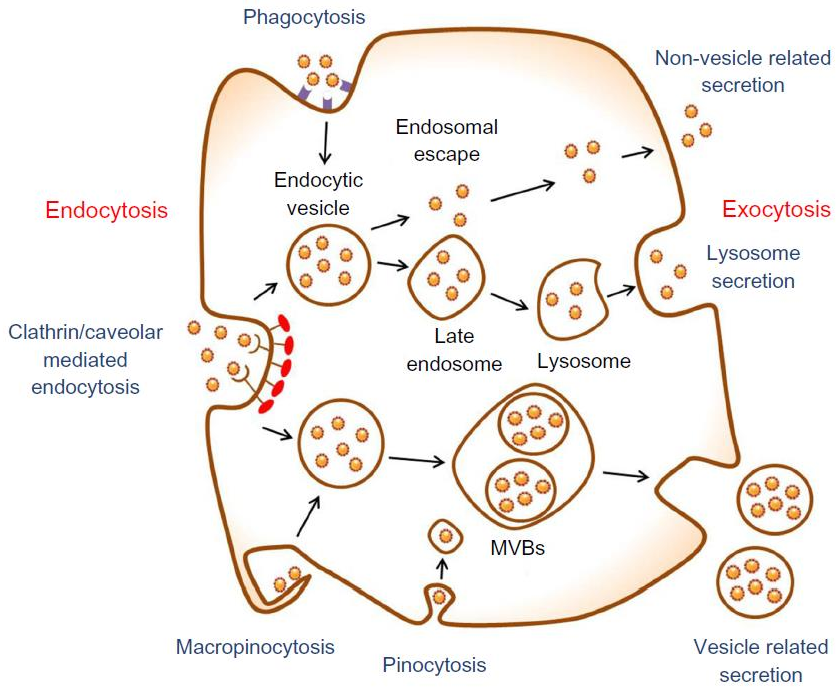

Figure 3: Schematic representation of possible exocytic mechanisms involved in nanoparticles exocytosis (MVBs – Multivesicular bodies)(Oh & Park, 2014)

Some materials, potentially including nanoparticles, are capable of so called endosomal escape. Endosomal escape means that the material engulfed in early endosome can elude into cytosol. Stayton et al. proposed that this escape is highly important in respect of cytotoxicity, as nanoparticles situated freely in cytosol tend to remain there and are unlikely to leave the cell (Stayton et al., 2009). In this case, the biocompatibility of silicon based nanoparticles may be an interesting advantage.

Yanes et al. demonstrated, that their mesoporous silicon nanoparticles are released from cells by lysosomal exocytosis, which is commonly being related to cellular stress response (Yanes et al., 2013). Interesting experiment was conducted by Slowing et al. They showed cells using transcytosis of mesoporous silica nanoparticles and also that the exocytosis itself is cell type dependent (Slowing et al., 2011).

The significant lack of studies and information might be caused by the challenging nature of this field. The exocytosis can be studied by live cell imaging, which, however, requires additional fluorescent labelling or structures that already possess strong enough fluorescence of its own to avoid photobleaching. Fluorescence related is also flow cytometry

quantification of cells with nanoparticles. Other option is then quantification of nanoparticles amount in supernatant, however, this could be quite challenging approach, as the identification itself cannot be precise.

Without any doubt, deeper understanding of exocytotic mechanisms deployed in respect to nanoparticles is needed for their future possible use in biomedicine.

4. Materials and Methods

If not stated otherwise, all percentages represent volume.

4.1. Cell Culture

All work relating cell cultures was conducted in sterile environment (hooded flow box, Scholler Instruments).

4.1.1. Cell Lines and Cultivation Conditions

Two different cell lines were used in this study – human osteoblast cell line SAOS – 2 (gift from Dr. Ute Hempel, Technische Universität - Dresden) and human monocyte cell line THP-1 (ATCC).

4.1.2. Subculturing

The cells were normally cultured in 75 cm^2 culture flasks (Techno Plastic Products AG) in standard cultivation medium – McCoy's 5A medium (GE Healthcare – HyClone) for osteoblasts and RPMI 1640 medium (Biowest) for monocytes – supplemented with 15 or 10 % FBS (Life Technologies) respectively, L-glutamine (Life Technologies) and 10 000 U/ml penicillin and 10 µg/ml streptomycin (both Sigma-Aldrich) at 37°C, 5% CO_2 atmosphere incubator (Thermo Fisher Scientific).

Both cell types were subcultured using following methods. Cells were harvested using furtherly described methods and an approximate count of 500 000 – 1 000 000 cells was returned to the previously used 75 cm^2 culturing flask providing fresh standard cultivation media up to volume of 10 ml.

Harvesting procedure for experimental use of adherent cells was using pre-wash by 5 % ethylenediaminetetraacetic acid (EDTA, Thermo Fisher Scientific - Gibco) in phosphate-buffer-saline (PBS, Thermo Fisher Scientific – Gibco, 10 times diluted prior to usage) and subsequent 5 – 10 minutes incubation with 0.1 % Trypsin in EDTA/PBS solution (1 ml/cultivation flask, Thermo Fisher Scientific - Gibco). The reaction was stopped by addition of 4 ml of respective medium. Harvesting of suspension THP-1 cells did not require any special technique.

4.1.3. Freezing and Thawing of Cells

For freezing, cells were harvested in exponential growth phase and a count of approximately 1 000 000 – 2 000 000 cells per cryogenic vial (800 µl) was used. The cells were then centrifuged (5 minutes, 150 g, at room temperature (r.t.)) (Hettich Universal

320 R). The supernatant was discarded and pellet was resuspended in adequate amount of cultivation medium. Further, 800 µl of cell suspension was transferred to cryogenic vial and 100 µl of foetal bovine serum (FBS, Thermo Fisher Scientific – Gibco) and 100 µl of dimethyl sulfoxide (DMSO, Sigma Aldrich) was added into the cell suspension. Immediately after this the cells were transferred in freezing container (CoolCell, BioCision) for overnight freezing in -80°C prior to long term storage in liquid nitrogen.

For thawing, freezed vial was removed from liquid nitrogen and thawed rapidly (1 minute, 37°C) and diluted in 9 ml of pre-warmed cultivation medium. The cells were then centrifuged (5 minutes, 150 g), supernatant was discarded and cells were diluted in fresh medium and transferred to cultivation flasks. The cells were cultivated for one week prior to experimental usage.

4.1.4. Experimental Conditions

For experiments, the cells were harvested at 70 – 90 % confluence and seeded in concentrations of 10 000 cells/cm^2 for SAOS-2 and 25 000 cells/cm^2 for THP-1.

In case of cytotoxicity experiments, the cells were seeded on 96-well plates (Techno Plastic Products AG).

In case of imaging, the cells were seeded on cell-imaging 4 to 8 well glass or plastic bottom dishes (Thermo Fischer Scientific - Labtek).

For all experiments with SAOS-2 cells, the standard cultivation medium (McCoy's) was replaced by Dulbecco's Modified Eagle Medium (DMEM, Thermo Fisher Scientific - Gibco) and only 5 % FBS supplementation (otherwise supplemented in the same way as standard cultivation medium). In this case, prior to addition of DMEM medium, cells were washed with pre-warmed PBS. This step has been included to eliminate formation of particle clusters caused by biomolecules from cultivation environment.

To run the experiment with "naked" nanoparticles cultivation medium not supplemented with FBS was used. In this case, cells were exposed to nanoparticles in FBS – free medium but in respect to maintain the cell viability, after 6h of incubation FBS was added to reach the final concentration of 5% FBS in the medium.

4.1.5. Doubling Time Establishment

In order to characterize used cell lines, doubling time was established for both of them. Initial concentration of 15 000 cells / cm^2 for SAOS-2 cell line and 25 000 cells / cm^2 for THP - 1 cells was seeded on 6-well dish. After 4, 24 and 48 hour, two wells were harvested and counted. The obtained data were analyzed using computation website http://www.doubling-time.com/compute.php?lang=en (Roth V., Doubling Time Computing).

4.1.6. Differentiation of THP-1 Cells

THP-1 cell line can be cultivated in two stages. As suspension of monocytes, which is its natural state, or as adherent and possibly differentiated macrophages. The differentiation itself is performed by 72 hours long stimulation of monocytes by phorbol 12-myristate 13- acetate (PMA, Sigma-Aldrich) diluted in DMSO in 100 nM concentration in standard cultivation medium. In order to work properly, the cells had to be seeded for differentiation at concentration of 160 000 c/cm^2.

4.2. Particle Characterization

Several types of particles originating from three different collaborating groups were used for this study.

Firstly, particles called silicon quantum dosts (**SiQDs**) originating from group of Dr. Minoru Fujii (Department of Electrical and Electronic Engineering, University of Kobe) were used. These particles compose of silicon (Si) co-doped with boron (B) and phosphorus (P) and poses the standardized diameter of approximately 4 nm. Due to the co-doping with B and P, the particles are fully soluble in water solutions and possess natural fluorescence (excitation approximately 405 nm and emission in range of 700 – 850 nm). These particles were supplied as transparent orange solution in methanol with concentration of 1 400 µg/ml. Before addition to cells, desired amount of particle solution and equal amount of distilled water were evaporated in dry bath set to 70°C until half of the liquid was evaporated and thus nanoparticles were transferred into water.

Secondly, particles called **SiC** due to their composition which were prepared by the group of Dr. Adam Gali (Hungarian Academy of Sciences) were used. The particles are composed of Si and carbon (C) and their diameter ranges from 2 – 5 nm. These particles as well possess natural fluorescence (excitation approximately 320 nm and emission in range

of 400 – 600 nm). Particles were supplied as transparent orange solution in water with concentration of 10 000 µg/ml and were filtered using 0.22 millipore filters (Techno Plastic Products AG) prior to use.

Thirdly, particles with code name **SiNP** prepared by the group of RNDr. Kateřina Herynková, Ph.D. (Department of Thin Films and Nanostructures, Czech Academy of Sciences) were used. These porous silicon particles formed approximately 100 nm clusters with fluorescence wavelength peak emission at about 650 nm and excitation at 405 nm. The particles were prepared in three different solutions to stabilize their solubility - in water, bovine serum albumin (BSA, Sigma Aldrich) and glycine (Sigma Aldrich). Particle code name followed by storage solution name has been used – SiNP – H_2O, SiNP – BSA and SiNP – Gly, respectively.

4.3. Determination of Metabolic Activity

Metabolic activity of the cells after incubation with particles was measured using either CellTiter® Aqueous One Solution Cell Proliferation Assay (MTS, Promega Corporation) or alamarBlue® cell viability reagent (AlamarBlue, Invitrogen).

MTS assay is a colorimetric method based on reduction of yellow MTS (namely (3-(4,5-dimethylthiazol-2-yl)-5-(3-carboxymethoxyphenyl)-2-(4-sulfophenyl)-2Htetrazolium)) tetrazolium compound by NADP(H) dependent dehydrogenases in metabolically active cells into darkly colored formazan. Adherent cells after incubation with particles were washed with pre-warmed PBS and then 10 % solution of MTS in corresponding medium was added. The cells were then incubated for 2 hours in CO_2 incubator, from time to time shaken softly for even color distribution. After 2 hours, optical density was measured on microplate multidetector reader (Synergy 2, BioTek Instruments, Inc.) at 490 nm, subtracting the background at 655 nm. For results, adequate blanks were subtracted and the values were compared to corresponding controls (non-treated cells).

AlamarBlue kit possess the same principles and method as MTS assay, however it is not based solely on colorimetry but on fluorescence levels measurement (excitation at 520 nm and emission at 690 nm). Subsequently reference value is subtracted as background and results are processed in the same manner as using MTS assay.

In case of non-adherent THP-1 cells, the staining solution was directly added to the samples to form a 10 % solution without any washing step.

4.4. Apoptosis Detection

Detection of apoptosis was performed using M30 CYTO/Death (conjugated with fluorescein - FITC, PEVIVA AB). The principle of this method lays in specific fluorescence labeling of caspase-cleaved cytokeratin 18.

After incubation of cells with particles, the sample was washed with PBS (5 minutes, 3 times) and subsequently fixed in 4% paraformaldehyde (Sigma Aldrich) in PBS for 15 minutes followed by washing with PBS (5 minutes, 2 times). The cells were then treated with Triton X and blocked by 1% FBS and 0.05% Tween (Sigma Aldrich) in PBS for 30 minutes followed by washing with PBS. The fixed sample was then incubated with M30 dye (1:10 in blocking solution) for 1 hour (dark, 37°C). Samples were washed with PBS (5 minutes, 2 times) and cellular nuclei were stained by 4',6-Diamidino-2-phenylindole dihydrochloride (DAPI, Sigma Aldrich, stock concentration 1 mg/ml, 1:1000 in blocking solution) for 45 minutes at 37°C at dark.

The samples were then washed twice with PBS and analyzed using a fluorescence microscope (Nikon Eclipse Ti-S) and the images were processed using CellProfiler software (Imaging Platform, Broad Institute).

4.5. Lactate Dehydrogenase Assay

Lactate dehydrogenase (LDH) is present in all living cells and can be detected in culture media only when cellular membrane is compromised. The Cytotoxicity Detection Kit (LDH, Roche applied sciences) works on similar principle as previously described MTS assay i.e. reduction of tetrazolium compound.

Positive control was aquired by addition of 10 µl of 100% Triton X to wells marked as dead control. Supernatants discarded from cell samples before preparation of MTS assay were transferred to 1.5 ml eppendorf tubes and kept in freezer prior to use. Then, the frozen supernatants were thawed slowly on ice followed by fast spinning (21 380 g, 10 minutes, 4°C). Meanwhile a new 96-well plate was prepared with 50 µl of PBS in each well and 50 µl of corresponding thawed and spinned samples (without any debris) were added. Subsequently 100 µl of LDH detection solution (5 625 µl of buffer and 125 µl of substrate per one plate) was added. The sample was incubated for 30 minutes at room temperature in dark place. After 30 minutes, 50 ul of stop buffer was added. Prior to measurement the plate was softly shaken for even color distribution and optical density was measured on

microplate multidetector reader at 490 nm, subtracting the background at 600 nm. Corresponding blanks were subtracted and the values were compared to corresponding controls.

4.6. Flow Cytometry

Characterization of THP-1 cells (both monocytes and PMA stimulated) was conducted using BD FACSAria Fusion cell sorter (BD biosciences) in collaborating laboratory (Biomedical center, Faculty of medicine, Pilsen). Cells were harvested by previously described methods and count of 500 000 cells in 100 µl of PBS was used for staining. Antibodies against specific markers were obtained as a gift from hematology department of University Hospital in Pilsen – Lochotin, Pilsen. Antibodies mentioned in table 1 were used for three separate experiments. Also another set of antibodies was tested, but proved to be less effective.

Marker	Antibody
CD14	APC-Cy7
CD16	FITC
CD64	APC
HLADR	PE

Table 1: Used markers for flow cytometry and corresponding antibodies

The cells were incubated with mixture of 5 µl of each antibody for 15 – 30 minutes in dark at room temperature. After staining the solution was washed in WASH solution (PBS with 2% FBS), then the cells were centrifuged (210 g, 5 min) and the pellet was resuspended in 200 µl of PBS and 10 000 events were measured.

Data were processed using FlowJo software (FlowJo LLC).

4.7. Fluorescence Staining

For colocalization studies, SAOS-2 cells were seeded on Ependorf Cell Imaging Coverglass with 8 chambers and incubated with particles for different time points. Subsequently, medium containing particles was discarded and cells were washed with PBS (5 minutes, 3 times). After washing the cells were fixed in 4% paraformaldehyde (Sigma Aldrich) in PBS for 15 minutes followed by washing with PBS (5 minutes, 2 times). The cells were later treated with 0.1 % Triton-X 100 (Sigma Aldrich) in PBS for 20 minutes followed by two washing steps. Then, the cells were blocked in 1% FBS and 0.05% Tween (Sigma Aldrich) in PBS for 30 minutes and again followed by two washing steps. Primary antibodies diluted in blocking solution according to dilutions in table 2 were incubated with fixed cells for

1 hour in dark at 37°C. Secondary antibody diluted also as described in table 2 was kept for 45 minutes at 37°C. The staining steps were separated by 3 washing steps.

Primary antibody (all Abcam)	**Dilution in blocking solution**
mouse monoclonal antibody anti EEA1 (early endosome)	1:100 (stock conc. 1 mg/ml)
mouse monoclonal antibody anti M6PR – cation independent (late endosome)	1:200 (stock conc. 1 mg/ml)
mouse monoclonal antibody anti LAMP 2 (lysosome)	1:50 (stock conc. 0.1 mg/ml)
Secondary antibody (Thermo Fisher Scientific)	**Dilution in blocking solution**
secondary antibody goat anti mouse AF568	1:1000 (stock conc. 2 mg/ml)

Table 2: Dilutions of antibodies for fluorescent staining

After completing the staining procedure cells were washed 3 times with PBS and mounted in moviol (Thermo Fischer Scientific) on deck glass. Samples were then kept for drying in fridge for at least 48 hours.

Additionally in some experiments the cellular nucleus was stained with DAPI. In experiments using DAPI, its dilution of 1:1000 (stock concentration 1 mg/ml) was added to samples at the same time as secondary antibody and was incubated for the same period of time at the same conditions.

4.8. Microscopy

Samples were observed using two different confocal microscopes, Leica TCS SP8X (Leica Microsystems) using Leica DFC365 FX monochrome digital CCD camera and Olympus IX83 (Olympus) with DS-Qi1Mc digital camera (Nikon), both using Nomarski (DIC) contrast by magnification objectives of 63 (HC PL APO CS2 63x/1.40 OIL objective). The microscope settings is described in table 3. Data were processed for smoothness and contrast correction using ImageJ software with Bio-formats plug in (Research Services Branch, National Institute of Mental Health).

Leica TCS SP8X settings	
SiQD particle detection	Excitation: 475, 483, 491, 499 nm (white light laser, pulse with 5-12 ns gating) Emission: 700- 795 nm (hybrid detector HyD3)

	100% gain, 10x line accumulation, 48.83 µs pixel dwell time (speed 10)
Antibody detection	Excitation: 568 nm (white light laser, gating 3-12 ns) Emission: 590 – 620 nm
SiNP detection	Excitation: 405 nm (diode laser) Emission: 630 – 670 nm (hybrid detector HyD3) 100% gain, 1.2 µs pixel dwell time (speed 100)
Olympus IX83 settings	
SiQD detection	Excitation: 405 nm (diode laser) Emission: 700 - 775 nm (Cy5 filter) 2000 ms exposition time
Antibody detection	Excitation: 561 nm (diode laser) Emission: 609 - 654 nm 400 ms exposition time

Table 3: Settings for SiQD, SiNP and antibody

Furthermore, changes in cellular morphology were observed using bright field microscopy enhanced by phase contrast in cytotoxicity studies. Bright field images and some SiC images were taken on fluorescenc microscope Nikon Eclipse Ti-S with Nikon DS-Qi1Mc camera, and were processed via ImageJ software.

4.9. Two-Photon Excitation Microscopy

For detection of SiCs, laser scanning confocal/two-photon (2-photon) microscope Olympus FV1200 (Olympus microsystems) at collaborating facility at Institute of Organic Chemistry and Biochemistry, Laboratory of Advanced Optical Microscopy was used and the measurement was conducted by Josef Lazar, Ph.D. SiC particles were observed using excitation wawelenght 405 nm and emmision was acquired at 470 – 570 nm. SiQD were observed by using excitation wawelenght of 488 nm and emmision was acquired at 695 – 795 nm. Both particles were observed by 60x objective magnification.

4.10. Electron Microscopy

SAOS-2 cells were seeded on 60 mm petri dish (Techno Plastic Products AG) and incubated for 24 hours in standard cultivation medium. After 24 hours, the cells were washed with pre-warmed PBS and fresh medium supplemented with 15% FBS with 11 µg/ml of gold nanoparticles (100 nm in diameter, Department of Solid State Engineering, Institute of Chemical Technology in Prague) was added and incubated for another 24 hours. After

24 hours, the medium was discarded and cells were washed with PBS (2 times, 5 minutes). After washing, the cells were fixed with 0.3% glutaraldehyde in 0.1% cacodylate buffer in MilliQ water (both Sigma Aldrich) for 30 minutes at room temperature. Then the cells were scraped using cell culture scrapper (Thermo Fisher) to form big agglomerates and were centrifuged (170 g, 5 minutes) into 1.5 ml Eppendorf tube. The supernatant was discarded and cells were resuspended in fresh glutaraldehyde in cacodylate buffer. The cells were then transported on ice to Institute of Chemical Technology in Prague.

After transportation, the cells were rinsed (centrifuged at 850 g, 2 minutes, supernatant discarded, resuspended in fresh buffer) two times in 0.1 cacodylate buffer and one time at 1 520 g, 5 minutes. The pellet was then covered with 1.5 ml of 1% osmium in veronal buffer (Lonza), resuspended and kept for 1 hour at 4°C. After 1 hour, the sample was centrifuged (1 520 g, 5 minutes) and rinsed with veronal buffer twice. The supernatant was discarded and sample was covered in melted 2.5% low melting agarose (Thermo Fisher) and kept on ice for 10 minutes. The stiffed sample in agarose was then transferred to ethanol series (10 minutes in each concentration, concentrations: 30%, 50%, 70%, 90% and 100% ethanol respectively, Sigma Aldrich). The samples were afterwards mounted in resin (Agar Scientific).

SiQDs and SiC were observed on collaborating workplace at Institute of Biology and Medical Genetics, First Faculty of Medicine, using transmission electron microscope FEI Morgagni with CCD camera MegaView III (Olympus systems). For observation purposes, 3 µl of corresponding particles were put on transmission electron microscopy grid (Sigma Aldrich) and kept to dry out completely.

4.11. Statistical Analysis

If not stated otherwise, all presented data origins from three independent repetitions of stated experiment, all composed of at least triplicates. Presented data show results as means of all experiments with error bars representing standard deviations. Extreme and remote values were excluded by box graph formation. Shapiro-Wilk test was used for data distribution assessment. Non-parametric Wilcoxon matched pairs test was used to determine significant differences among the datasets from corresponding control. Comparison of each dataset among each other was performed using ANOVA. Significance was set as P values of 0.5 and less. These analyses were performed using STATISTICA software (StatSoft, Inc.).

5. Results

5.2. Preliminary Results

Cellular behavior characterization is crucial before any material related experiments can be conducted.

5.2.1. Cell Characterization

Doubling time and basic metabolic activity test were determined for both cell lines used.

SAOS-2 - Human Osteoblastic Cell Line

Doubling time for this line was counted using computation website (http://www.doubling-time.com/compute.php?lang=en) from 4 time points and was found to be 43.11 hours and growth rate of 0.0161 (graph 1).

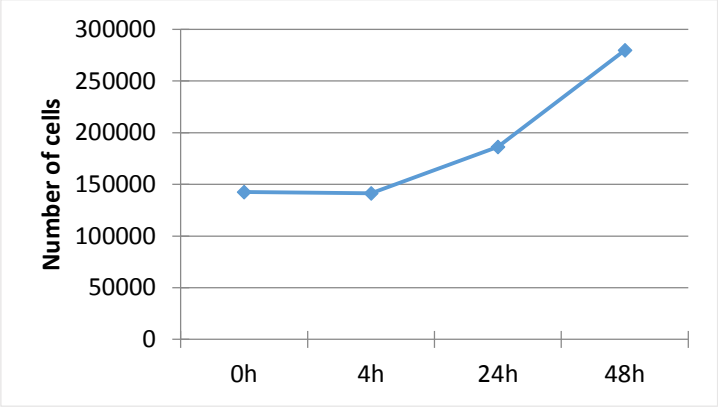

Graph 1: Graphic representation of cell growth for SAOS-2

Basic metabolic activity of different concentrations of SAOS-2 cell line was measured after 24 hours using MTS assay (graph 2).

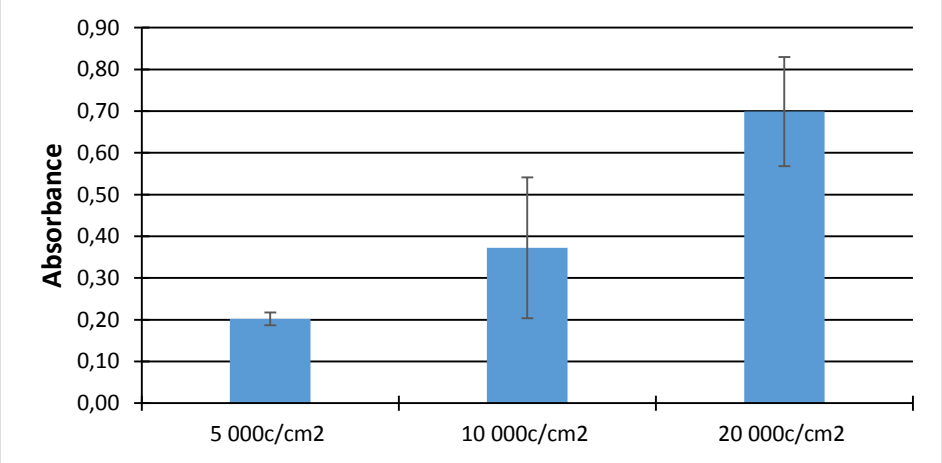

Graph 2: Absolute absorbance levels for SAOS-2 cell line at different concentration after 24 hours

THP-1 Human Monocyte Cell Line

Doubling time for this line in suspension of monocytes was counted using computation website (http://www.doubling-time.com/compute.php?lang=en) four time points and was found to be to 39.1 hours and growth rate of 0.0177 (graph 3).

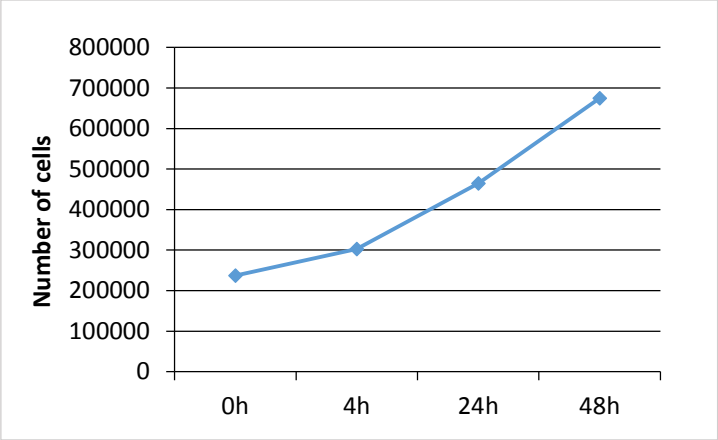

Graph 3: Graphic representation of cell growth for THP-1

Basic metabolic activity of different concentration of THP-1 cell line (monocytes) was measured after 24 hours (graph 4).

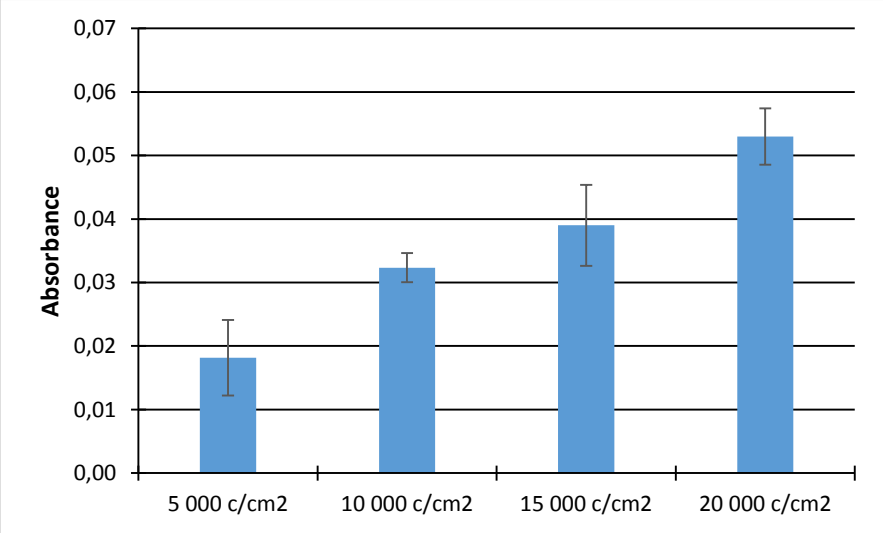

Graph 4: Absolute absorbance levels for THP-1 cell line at different concentration after 24 hours

In order to obtain adherent macrophage like cells, 72-hour stimulation with 100 nM concentration of PMA in medium was used. Differentiation experiments were conducted multiple times before achieving desired results. The PMA stimulated cells did not possess proper macrophage-like morphology when seeded in lower concentration (approximately 160 000 cells/well in 6-well dish). The seeding at higher concentration (typically 1 500 000 cells/well in 6-well dish) possibly provided enough cell-cell interactions, which

lead to proper morphology changes. The different morphology of monocyte and macrophage-like cells is demonstrated in Figure 4.

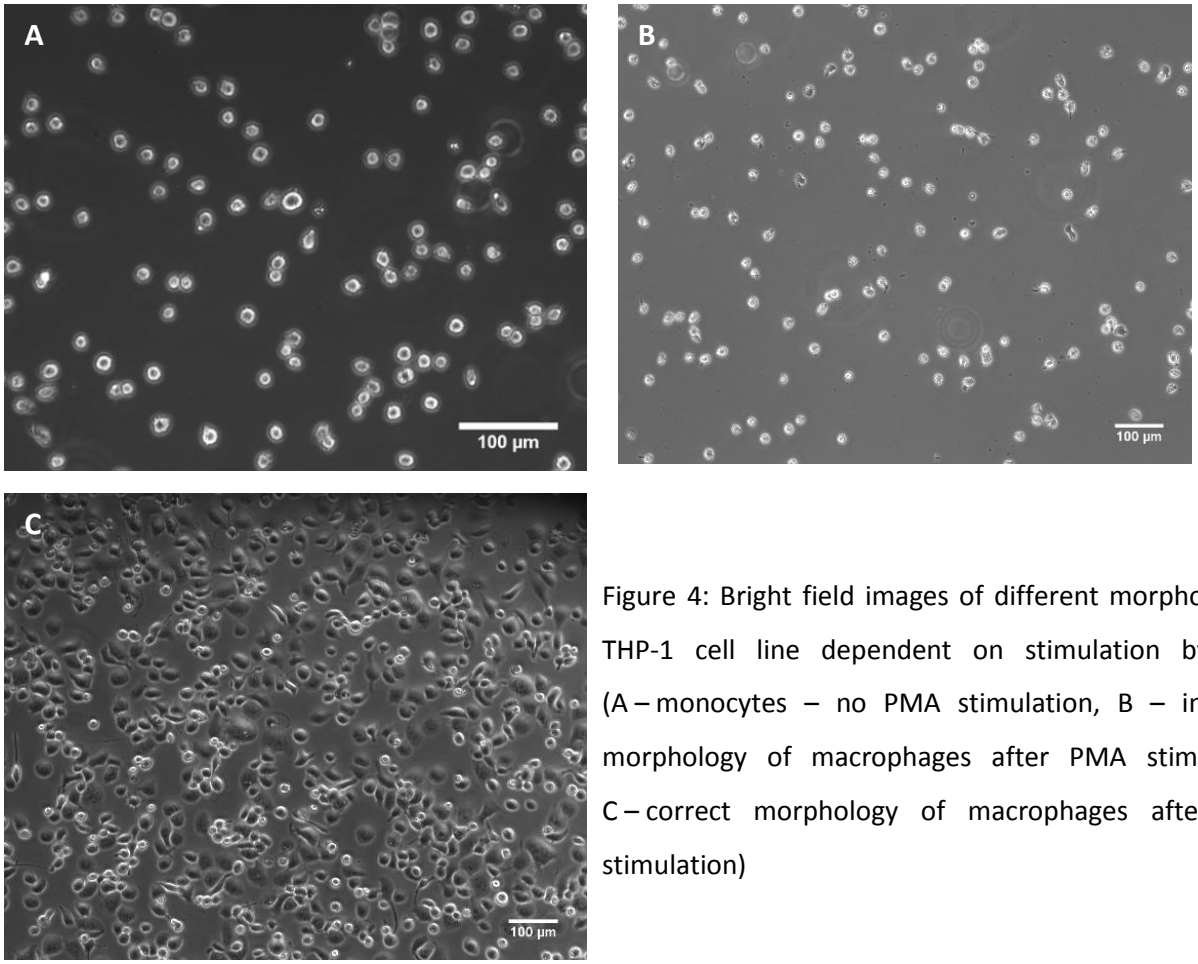

Figure 4: Bright field images of different morphology of THP-1 cell line dependent on stimulation by PMA (A – monocytes – no PMA stimulation, B – incorrect morphology of macrophages after PMA stimulation, C – correct morphology of macrophages after PMA stimulation)

In order to properly characterize the cells after stimulation with PMA, not only bright field microscopy was used but also flow cytometry measurements were performed to identify macrophage or monocyte markers. The flow cytometry experiments were conducted in total three times. Each time different results were obtained. The expression of four markers (CD14, CD16, CD64 and HLA-DR) was determined. According to BD protocols, monocytes should be CD16, CD14 and HLA-DR positive and CD64 negative, macrophages should be CD16 negative and CD14, CD64 and HLA-DR (less than monocytes) positive. Despite these information, our results proved to be inconsistent and do not comply with the above-stated.

Our results showed certain shift in positivity/negativity (only negative gating was used) in time (fig. 5A and 5B). It can be caused by passage number and sub culturing conditions. Overall, the only thing that can be taken for granted is that PMA stimulation changes the

granularity and size of the cells (fig. 6). Due to these results, THP-1 cells after PMA stimulation are not called macrophages in this study.

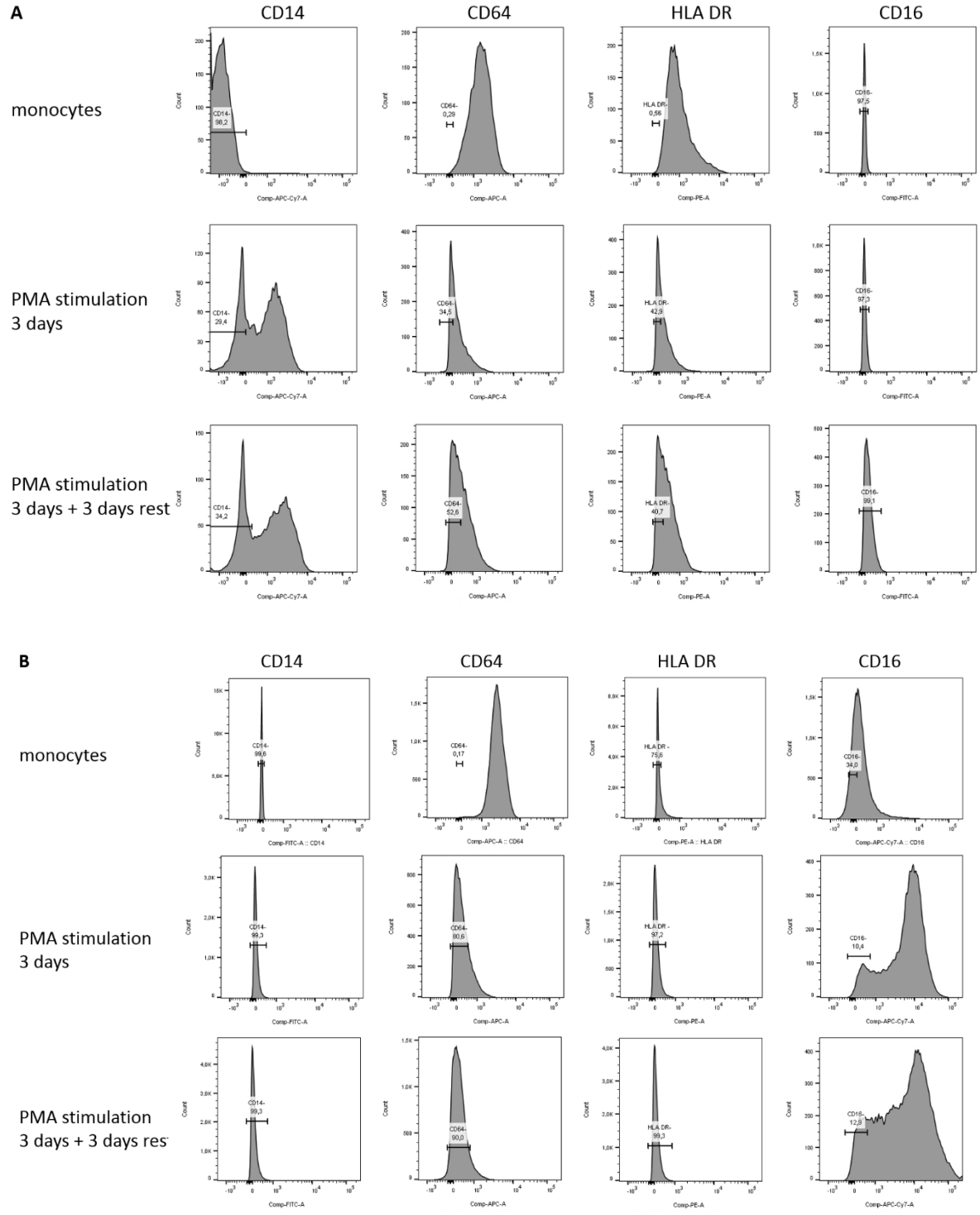

Figure 5: Flow cytometry data showing expression of markers on THP-1 cells shifting in time in two separate experiments A and B (the data were taken 4 weeks apart)

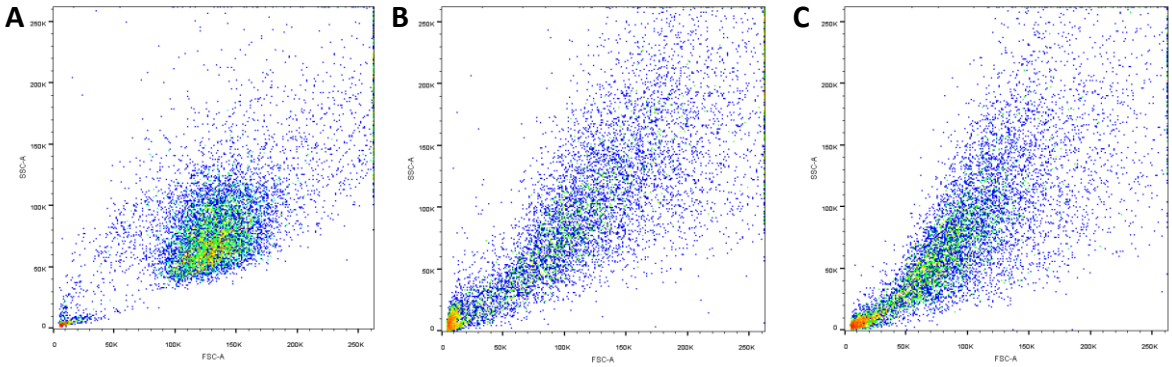

Figure 6: Forward scatter (FSC) and side scatter (SSC) distribution of each type of THP-1 cells (A – monocytes, B – 3 days stimulation with PMA, C – 3 days stimulation with PMA + 3 days rest)

5.2.2. Cultivation Conditions Establishment

As mentioned in literature overview, the impact of biological environment on behavior of nanoparticles is highly significant. The influence of different cultivation conditions on interaction of cells with nanoparticles was tested. The formation of biomolecular corona can be correlated with the presence or absence of sera in cultivation media. In order to identify possible influence of simple change in supplementation amount or type of sera used on cellular viability, or more precisely, the activity of mitochondria, MTS assay was conducted. SAOS-2 cells were incubated for 2, 6 and 24 hours in McCoy's medium supplemented with antibiotics, glutamine and different serum - foetal bovine serum (FBS) in concentration of 5 or 15 %, heat inactivated (30 minutes, 56°C) or non-inactivated and human plasma serum (HPS) - either mix of donors or only donor with AB blood type at the same concentrations as FBS, again thermally inactivated and non-inactivated. Medium with 15 % non-inactivated FBS established at our laboratory as standard cultivation conditions for these cells, was used as a positive control (100%) and to its value the other values were related. As SAOS-2 cell line is human osteosarcoma derived line, usage of human plasma serum was tested in order to simulate *in vivo* conditions of nanoparticle-proteins interactions.

According to our results, human sera, no matter what concentration or heat-treatment, significantly lowered cellular metabolic activity (Graph 5). The most important finding is

that lowering the culturing FBS concentration from 15 % to 5% does not affect the cells significantly. The results are, however, only from limited time of cultivation. Long-term cultivation with lowered FBS supplementation may lead to further effects.

Using these results as basis, all further nanoparticle related experiments use media with 5 % FBS, which is not harmful to the cells on one hand and on the other hand most probably lessens the formation of biomolecular corona.

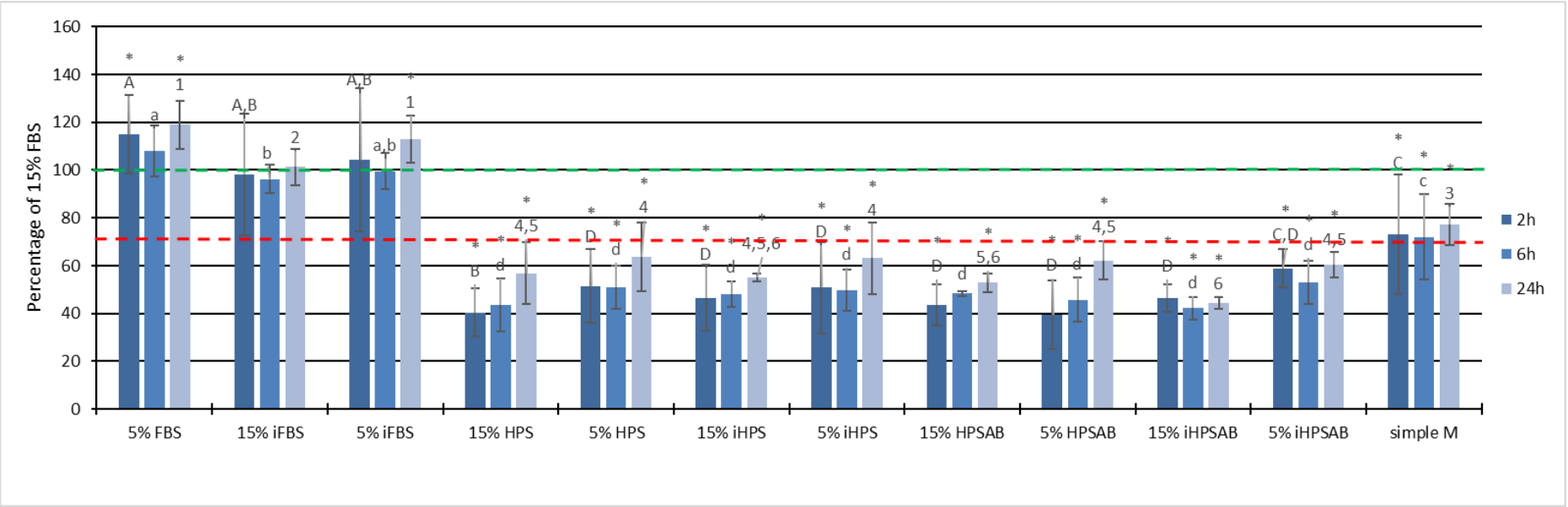

Graph 5: Metabolic activity of SAOS-2 cells determined after different time of treatment under different cultivation conditions. Values presented as percentage of cells under different conditions related to cells cultivated in medium supplemented with 15% FBS

Explanatory notes: FBS = foetal bovine serum, iFBS = foetal bovine serum heat inactivated, HPS = human plasma serum (mixed apheresis, ÚHKT), iHPS = heat inactivated human plasma serum (mixed apheresis, ÚHKT), HPSAB = human plasma serum from donor with AB blood type, iHPSAB = heat inactivated human plasma serum from donor with AB blood type

Statistics: As described in Materials and methods

Green line showing control level, red line showing cytotoxicity level of 75%

5.3. Cytotoxicity Experiments

The first thing to be done while working with any material in biology, is characterization of its impact on viability and fitness of the cells. In the following chapters the impact of each particles used will be showed and discussed separately. It is important to mention that each batch of any material might possess the same physicochemical characteristics, however, the cells can sense it differently. In all the experiments described below, the cells were seeded in 96-well dishes and exposed to gradually increasing concentration of particular nanoparticles (25, 50 and 100 μg/ml) in medium either supplemented with 5% FBS (expecting formation of protein corona on NP) or not supplemented with FBS (expecting no protein corona formation on NP) for first 6 hours. After this time, FBS was added to final concentration of 5% for rest of cultivation time to avoid deterioration of cell conditions.

5.3.1. SiQD (Japan)

Metabolic Activity Determination (MTS and Alamar Blue Assay)

As showed in chapter 4, MTS assay and Alamar blue assay possess similar principle and so the results can be showed and discussed together.

The particles provided from our collaborating group in Kobe came in several different batches. Even though the particles were fabricated in the same way and physico-chemical data provided were the same all the time, MTS test was conducted every time a new batch arrived. Surprisingly, the batches showed significant differences among each other.

For example, batch No. 1 showed small effects on SAOS-2 cell metabolic activity under conditions with 5% serum in the medium (graph 6A), but significant decrease of metabolic activity under serum-free conditions (graph 6B) in time as determined by MTS assay.

The graph 6B shows statistically significant increase in metabolic activity of cells exposed to SiQDs for 6 hours. This increase may be caused by the cells actively coping with bare nanoparticles entering cells. However, the cells were in longer time course harmed by these particles, which is apparent in significant decrease of their metabolic activity after 24 and 48 h. Thus, it could be concluded that the particles entering cells without biomolecular corona cause cytotoxic effects. According to literature, the cytotoxic level

means lowering of metabolic activity by 25% (Flahaut et al., 2006). This level is only achieved at concentration of 50 and 100 µg/ml SiQDs after 48 hours.

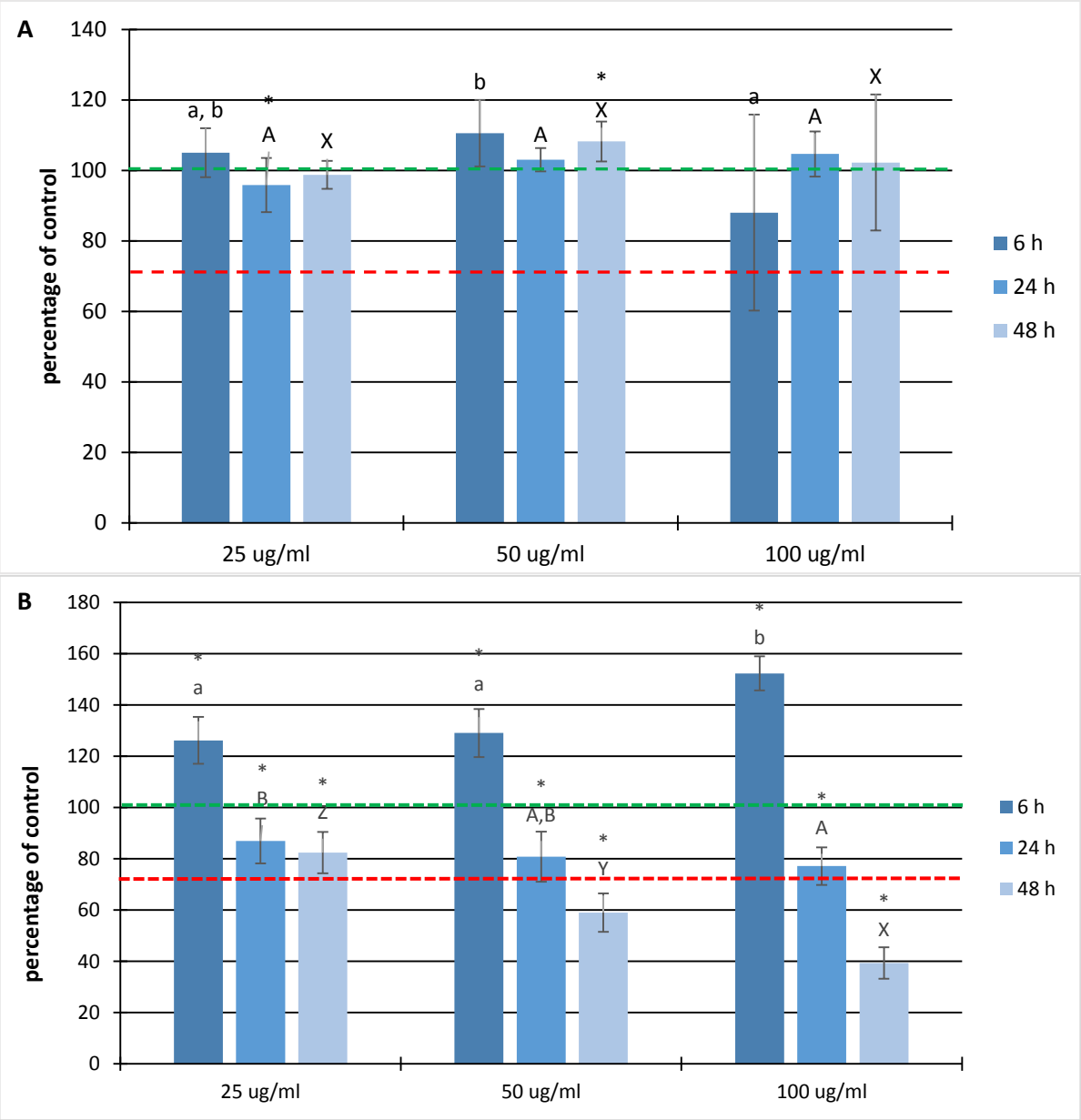

Graph 6: Metabolic activity of SAOS-2 cells measured by MTS assay in different time points with incresing concentration of SiQD batch No.1 (A – cultivation in medium supplemented with FBS, B – cultivation in serum-free medium)

Green line showing control level, red line showing cytotoxicity level of 75%

The batch No.1 was also used for metabolic activity measurements on THP-1 cells in both of their forms – suspension monocytes (THP-1) and adherent macrophages-like cells (THP-1 D). Since SiQD volume provided was limited, only two repetitions of this experiment were conducted at only two time points, however, each experiment was done in quadruplets to obtain enough data for statistics. Absolute numbers of absorbance could not be

compared while we test two completely different cell types (suspension and adherent cells). The percentage of control on the other hand is a number that can be compared.

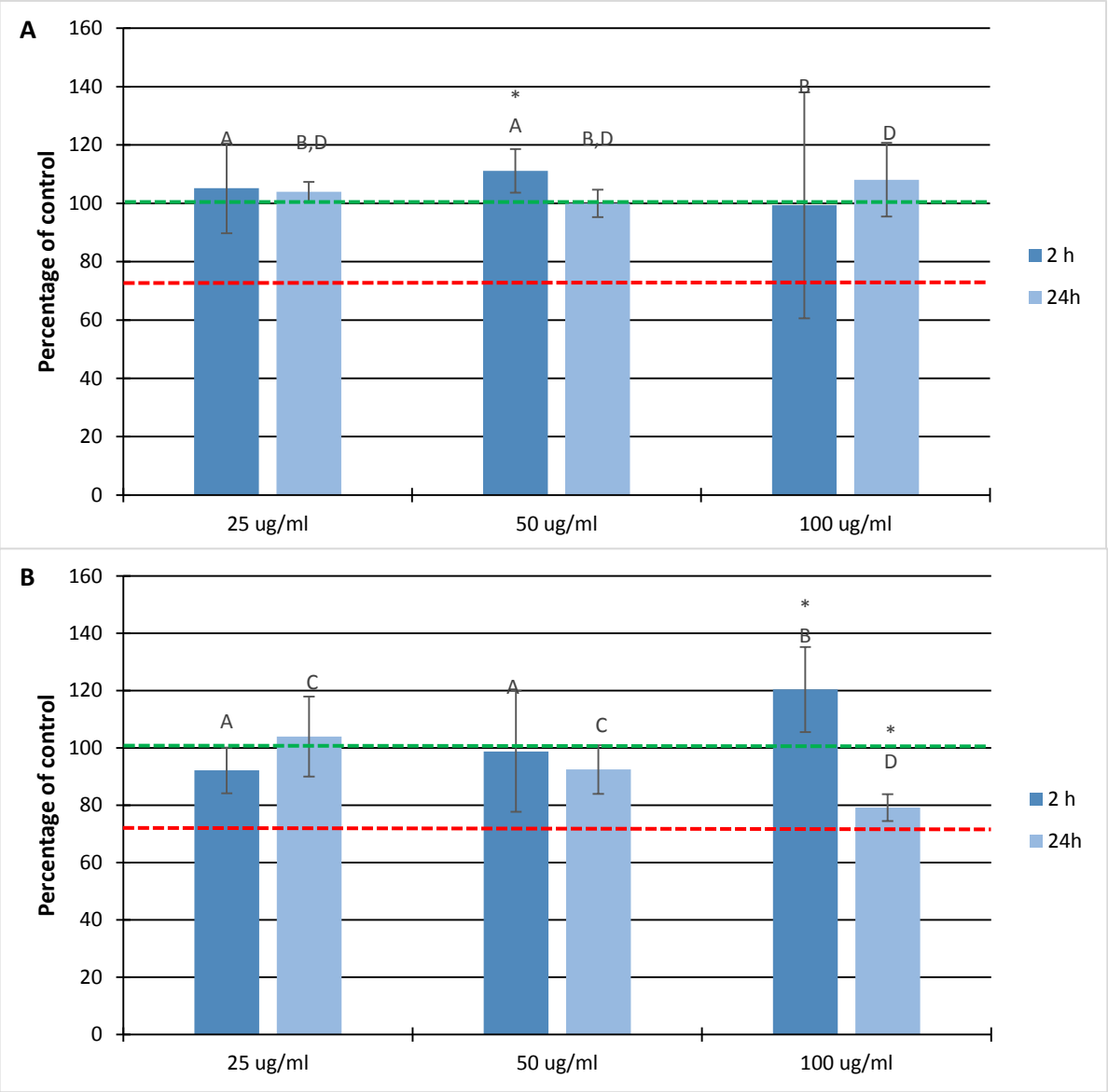

Graph 7: Metabolic activity of THP-1 cells measured by MTS assay at different time points with increasing concentration of SiQD batch No.1 in medium supplemented with FBS (A – THP-1 in suspension form, B – THP-1 D adherent form)

Green line showing control level, red line showing cytotoxicity level of 75%

As seen from graphs 7A and 7B, the SiQD (batch No.1) impact on THP-1 cells, both adherent and suspension, under conditions with FBS presence is not extensive. The significant differences shown in graphs might be caused by limited numbers for statistical evaluation and even when taken seriously, no decrease under 75% of control is present.

The results from serum-free media (graph 8A and 8B) again show slight increase of metabolic activity within first hours of cultivation, but only in suspension THP-1 cells. The trend of decreasing metabolic activity seen in SAOS-2 is present again. It may even seem like the reaction of THP-1 cells is more dramatic as the cytotoxic level of 75% of control is exceeded after 24 hours in all cases except for the lowest SiQD concentration in suspension form of THP- 1. This may be caused by the fact that immune cells tend to react more to unfamiliar particles in their environment.

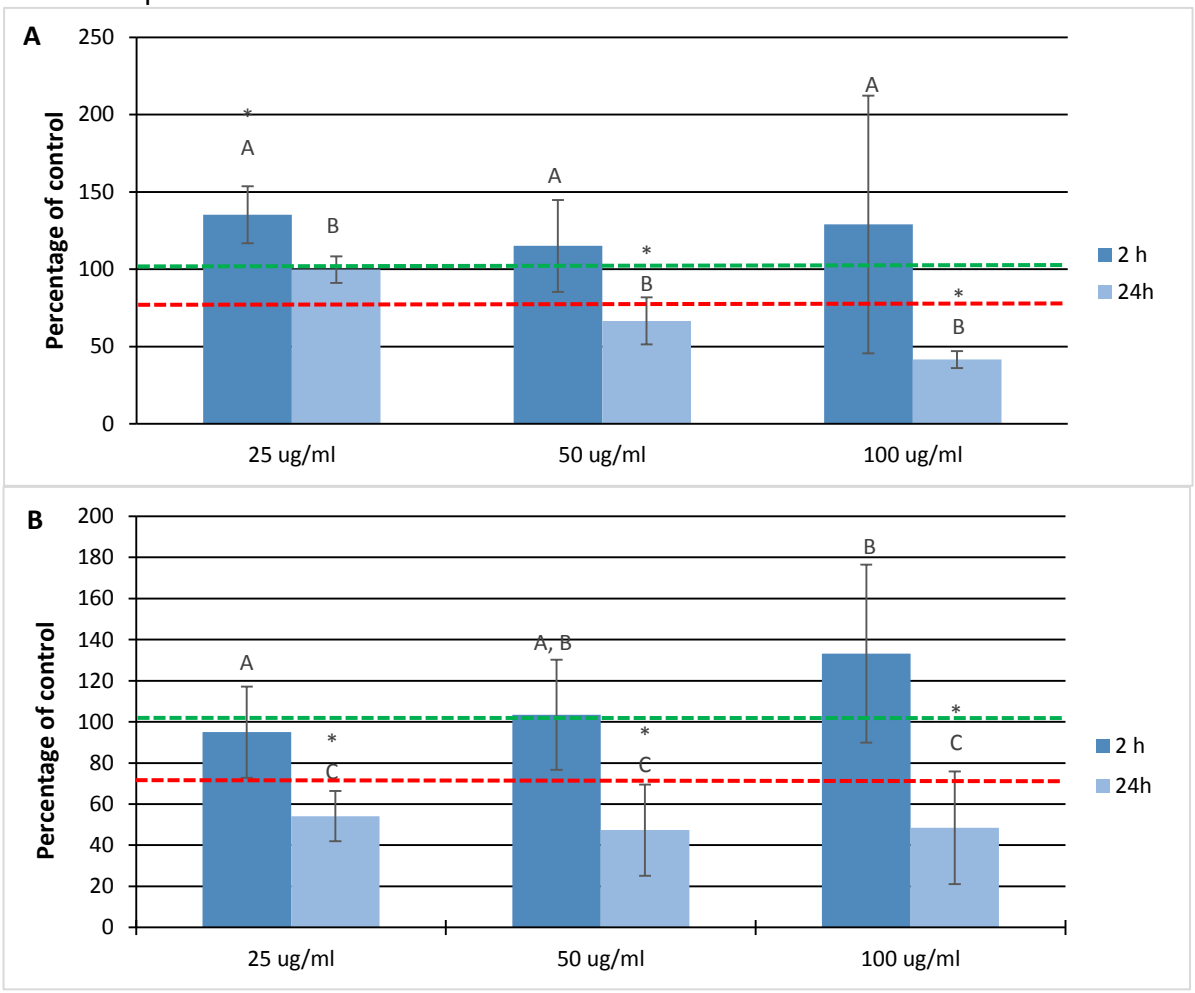

Graph 8: Metabolic activity of THP-1 cells measured by MTS assay at different time points with increasing concentration of SiQD batch No.1 in serum free medium (A – THP-1 in suspension form, B – THP-1 D adherent form)

Green line showing control level, red line showing cytotoxicity level of 75%

However, other batch, batch No.2 tested with monocytic THP-1 cells showed totally different results. The results from this batch could not be used, as particles immediately after addition of MTS solution started to interact with it, changed the color of the staining solution and thus provided false results (graph 9, fig. 8).

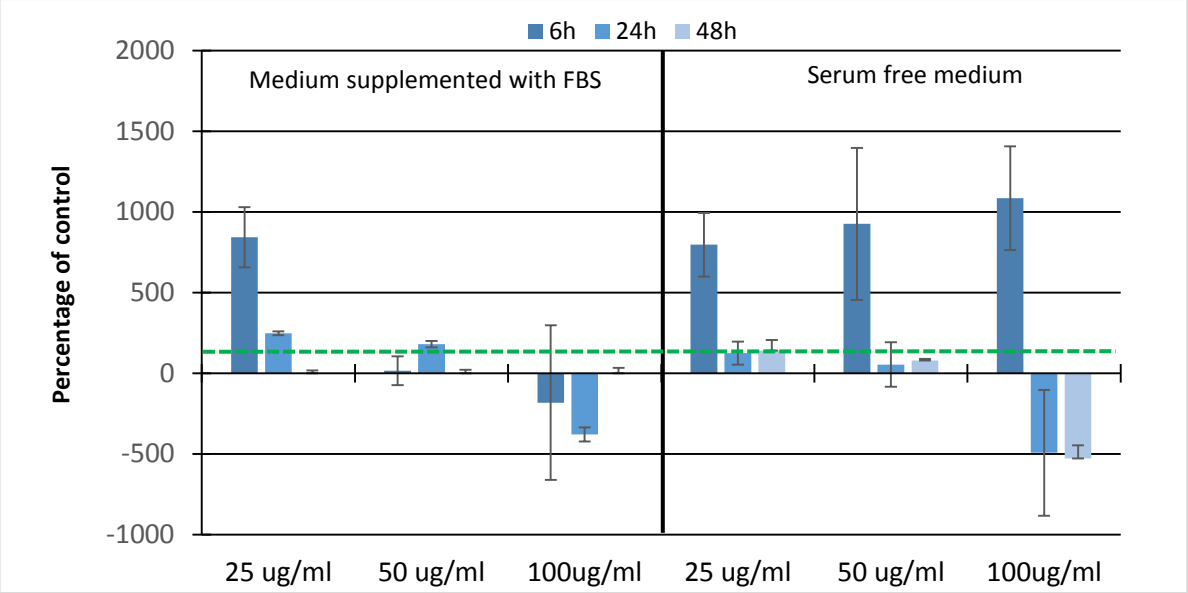

Graph 9: Metabolic activity of THP-1 cells measured by MTS assay at different time points with increasing concentration of SiQD batch No.2

Green line showing control level

Figure 8: Interactions of particles with MTS solution – circled out are blank wells containing medium with 50 µg/ml SiQDs (batch No. 2) without cells

To avoid this negative color change using MTS solution, we implemented new assay for determination of metabolic activity by using a fluorescence probe - Alamar blue assay (graph 10). However, upon fluorescence measurements, the results of blank with nanoparticles provided high fluorescence when compared to sample wells with cells. Regarding this, we deduced that this batch is unusable for further tests. The interactions with our implemented methods also suggested the interaction with cells might be completely different from previously used batch and replicable results would be hardly obtained.

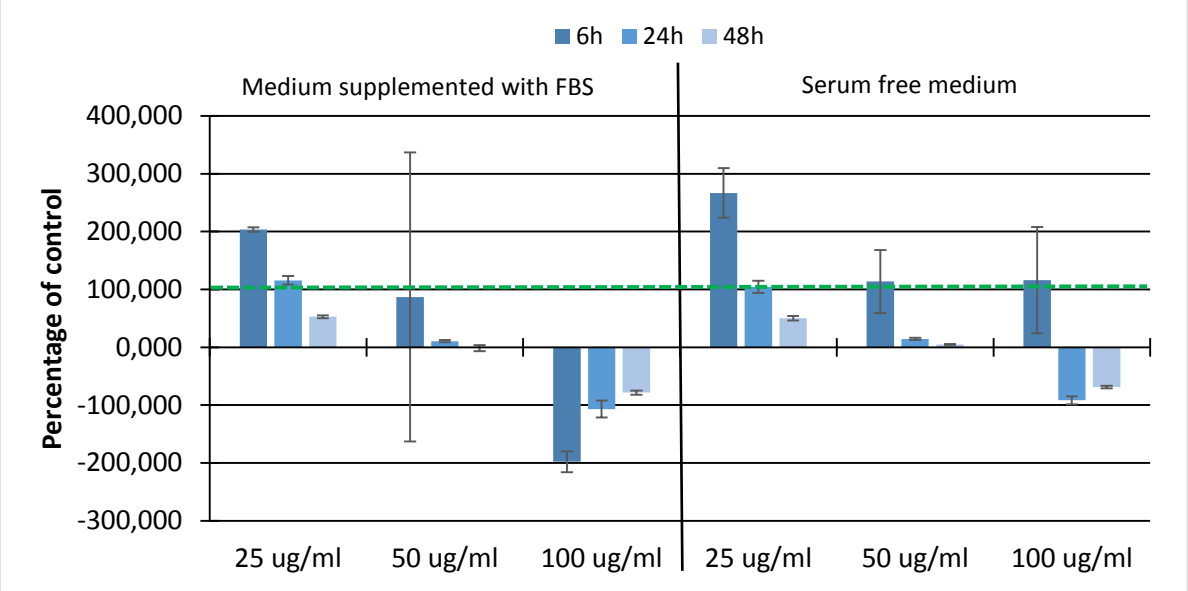

Graph 10: Metabolic activity of THP-1 cells measured by Alamar blue assay at different time points with increasing concentration of SiQD batch No.2

Green line showing control level

Recently, a completely new batch of SiQDs (batch No.3) was delivered. The results from this batch show similar trends and properties as batch No.1, only the concentration of 100 µg/ml seems to have stronger effect on SAOS-2 (graphs 11A and 11B). Again, in medium with serum, low concentrations of SiQD (25 and 50 µg/ml) have almost no effect. However, as stated previously, the highest used concentration of SiQDs shows rapid decrease in metabolic activity nearly to zero (visual confirmation of cell condition shown in fig. 9). We can see again the increase of metabolic activity after 6-hours incubation. MTS data shown for this batch originates from only two separate experiments, which did not provided enough data for proper statistical analysis.

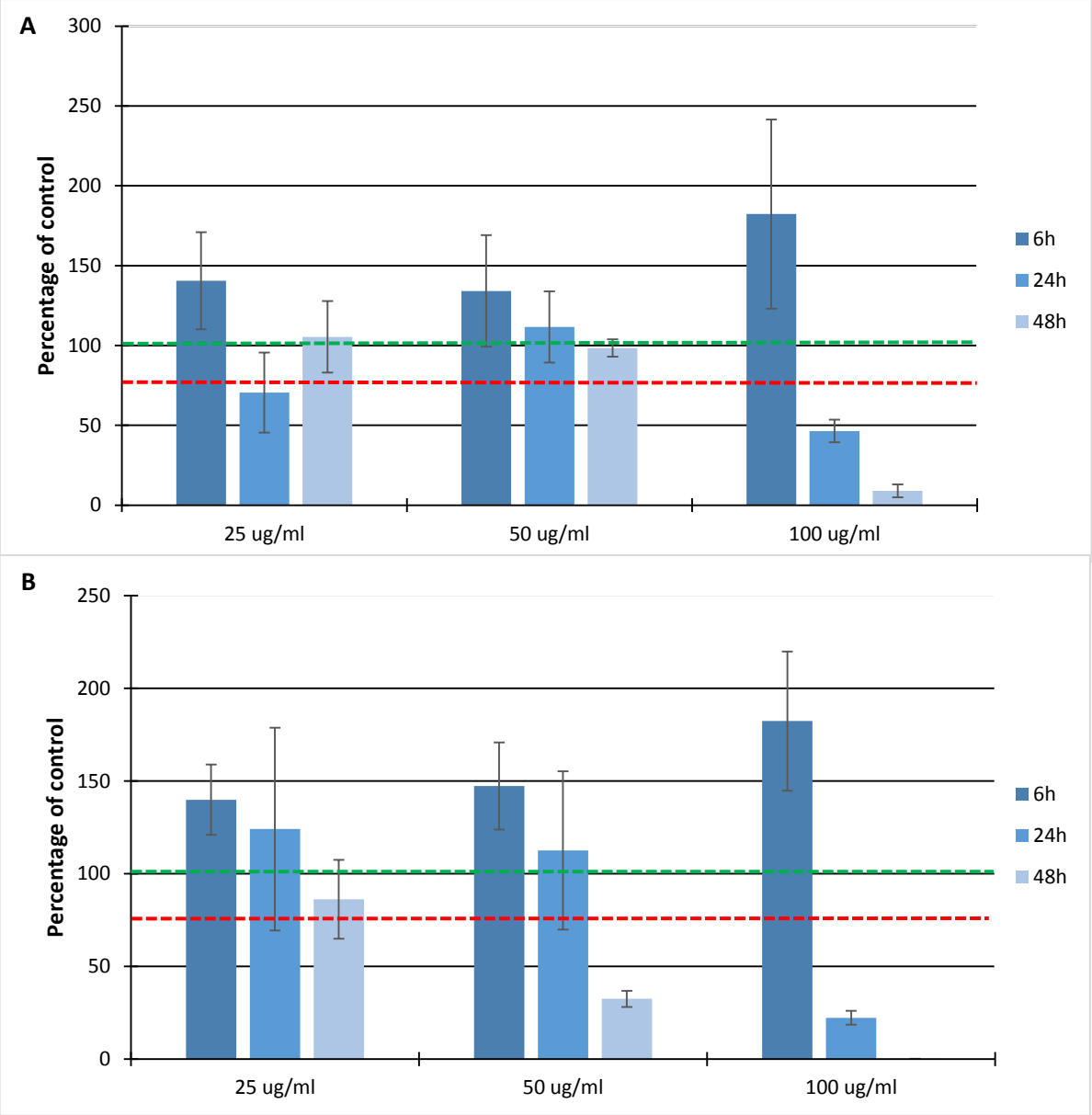

Graph 11: Metabolic activity of SAOS-2 cells at different time points with increasing concentration of SiQD batch No.3 (A – cultivation in medium supplemented with FBS, B – cultivation in serum free medium)

Green line showing control level, red line showing cytotoxicity level of 75%

Comparing all the results regarding metabolic activity measurements one can come to following conclusions. Any material that comes in different batches, even though its physicochemical characteristics seemingly remain the same, must be initially tested as seen on batch No. 2. The pattern showing possible significance of biomolecular corona formed based on FBS presence in the cultivation medium in SAOS-2 and THP-1 cells is clear. The presence of FBS lowers the negative impact of SiQDs on metabolic activity of both cell lines shown.

Necrosis and Apoptosis Detection

To accompany the previously shown results from MTS assay with further data and possibly identifying the mechanisms of impact of nanoparticles on cells, LDH assay as a necrosis-determining method was implemented. The principle of this method lays in detection of lactate dehydrogenase in supernatant, which is present there only upon plasmatic membrane rupture, typical for necrosis. For measurements, supernatants from cells used for MTS test of SiQD batch No.3 were used.

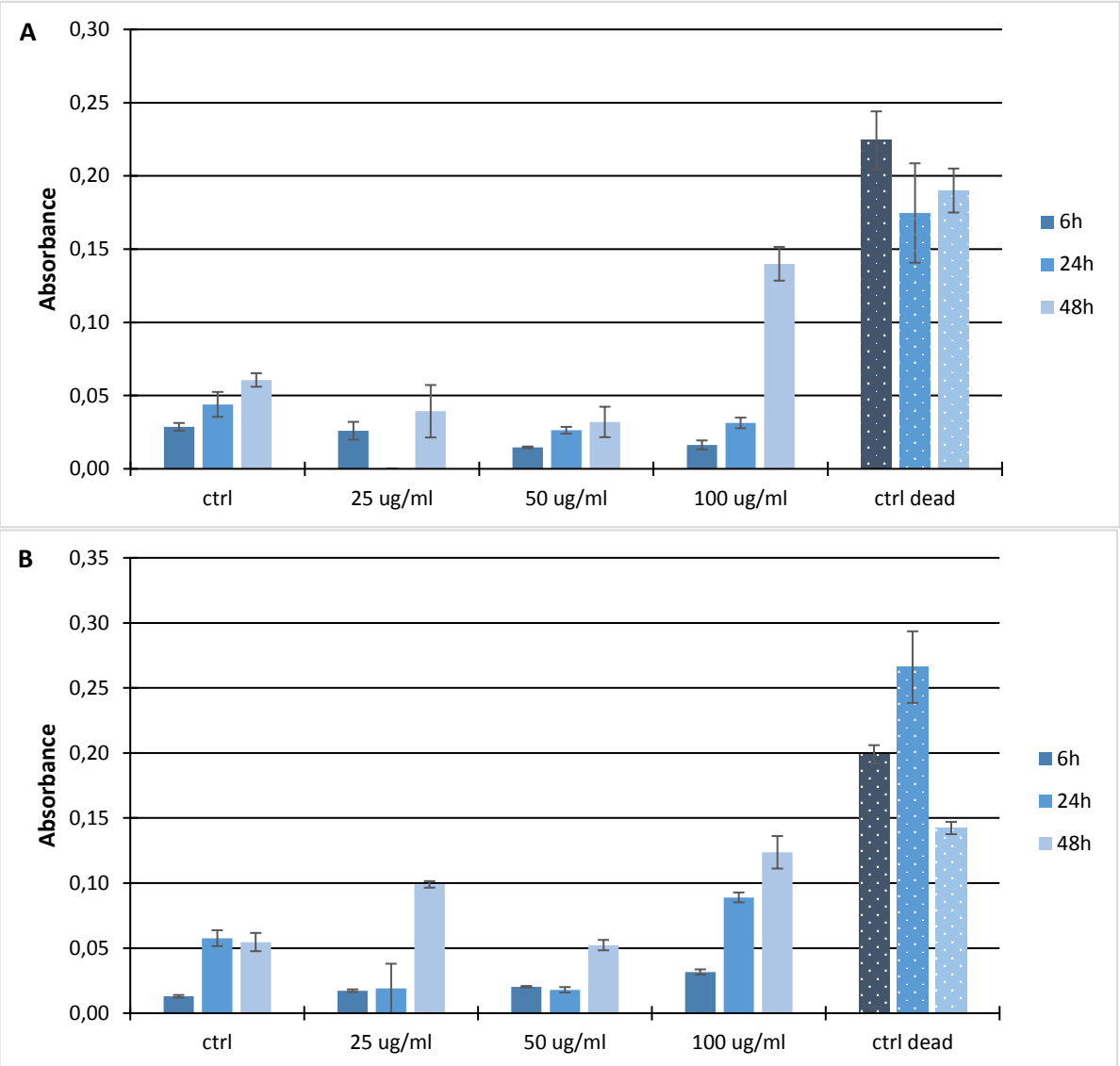

Graph 12: Detection of lactate dehydrogenase in supernatant of SAOS-2 cells incubated with SiQDs batch No.3 (A – cultivation in medium supplemented with FBS, B – cultivation in serum free medium)

Explanatory note: ctrl means control cells, ctrl dead means control cells where necrosis was induced by treatment with Triton X, no data were obtained after 24 hours at concentration of 25 µg/ml of SiQDs

From the results shown in graphs 12A and 12B, it is obvious that necrosis can be detected in cells treated with nanoparticles in serum-supplemented medium at highest concentration (100 μg/ml) only after 48 hours. At serum-free conditions, necrosis can again be detected only after 48 hours, but is visible at 25 and 100 μg/ml SiQD concentrations. The presented data originates from only one repetition of this experiment, so no relevant conclusions can be taken. However, it points the direction of our study as LDH is detected extensively in the medium of cells treated with high concentration of particles.

The MTS assay results showed decreasing metabolic activity also in the concentration 50 μg/ml of SiQDs in serum-free conditions after 48 hours, however nothing was detected by LDH assay. Due to this irregularity, detecting apoptosis as another possible way of metabolic activity interference was implemented with SAOS-2 cells. However, upon several unsuccessful attempts to stain apoptotic cells with M30 dye, we found out that presence of expression of cytokeratin 18 (the target protein for this assay) in other cells then single layer epithelial tissues is highly unlikely (Lauerová, Kovarik, Bártek, Rejthar, & Vojtěsek, 1988).

5.3.2. SiC (Hungary)

Metabolic Activity Determination (MTS assay)

As shown in graphs 13A and 13B the impact of SiC on SAOS-2 cell line seems to be nearly none in serum-containing conditions as well as in serum-free conditions. From this point of view these particles seem to be harmless at tested concentrations similar to concentrations of SiQD (Japan) and possess no significant impact on SAOS-2 cell line no matter what environment. Presented data originates from two separate experiments with not enough data to provide statistics.

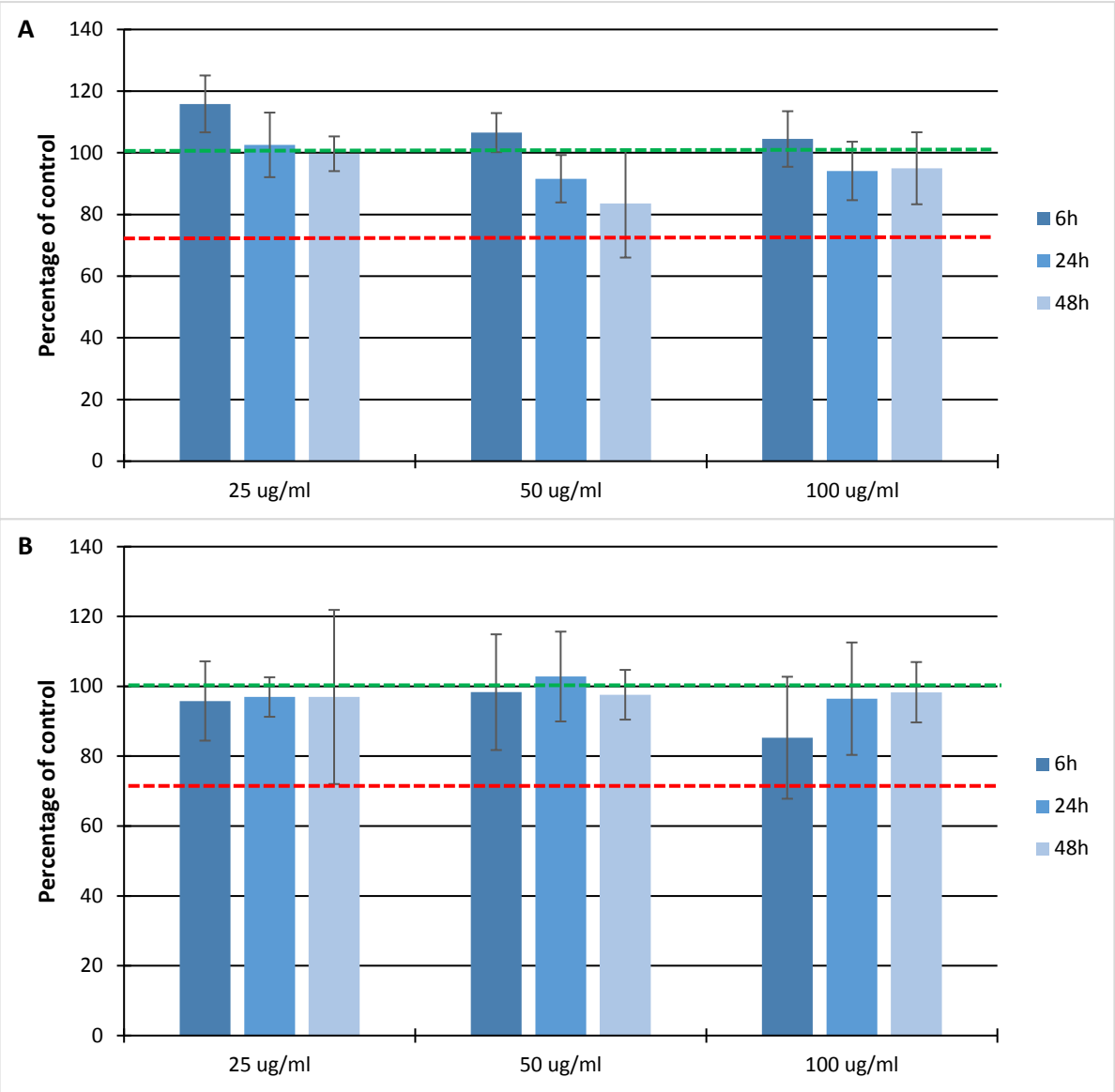

Graph 13: Metabolic activity of SAOS-2 cells measured by MTS assay at different time points with increasing concentration of SiC (A – cultivation in medium supplemented with FBS, B – cultivation in serum-free medium)

Green line showing control level, red line showing cytotoxicity level of 75%

The same particles were used also for MTS assay with THP-1 cells in adherent form (THP-1 D). With this cell type, completely different results were obtained (graphs 14A and 14B). Adherent form of THP-1 seemingly reacts on the presence of SiC in both media by lowering its metabolic activity. No change can be observed at the lowest concentration, however, higher concentrations show decrease to cytotoxic levels even after 24 hours. The reaction in serum-free conditions is only stronger, but shows simmilar trend. Again this experiment was conducted only two times so no statistics was performed.

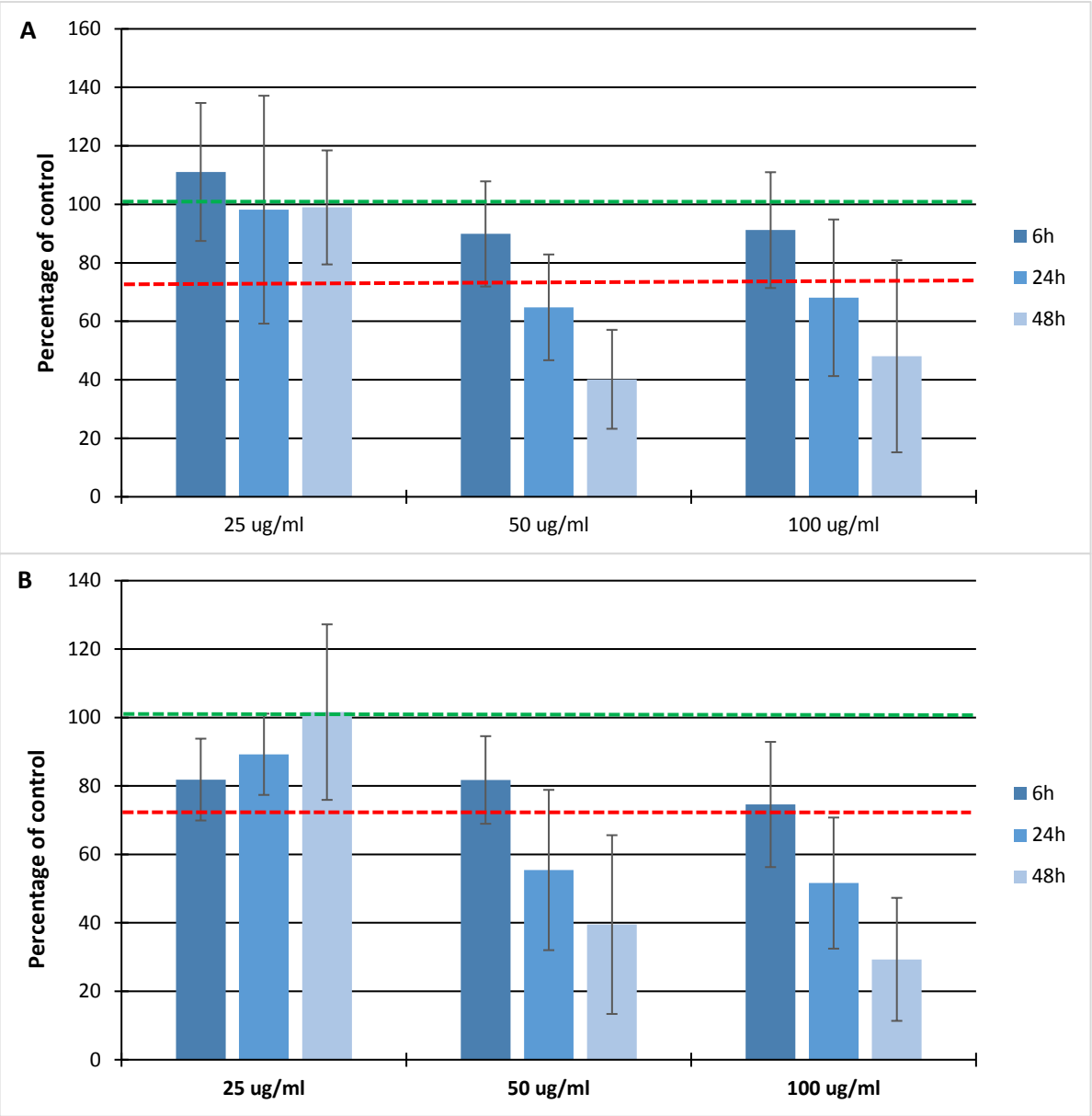

Graph 14: Metabolic activity of adherent THP-1 cells measured by MTS assay at different time points with increasing concentration of SiC (A – cultivation in medium supplemented with FBS, B – cultivation in serum-free medium)

Green line showing control level, red line showing cytotoxicity level of 75%

5.3.3. SiNP (Czech Republic)

Metabolic Activity Determination (MTS assay)

The SiC particles were provided as suspension in three different solutions – BSA, water and glycine. BSA and glycine solutions were used to stabilize the already existing agglomerates of nanoparticles and prevent them from further clustering whilst water solution was used as a reference. So far, just long term influence on metabolic activity of SAOS-2 cells was performed by MTS assay measurement after 48 hours incubation with

concentrations of 75, 100, 250 and 500 µg/ml of SiNPs in FBS supplemented medium. These nanoparticles proved to be less harmful than all previously showed as the only concentration to cause decrease below cytotoxicity level was 500 µg/ml (graph 15). The cytotoxic level was also exceeded by 250 µg/ml of glycine treated nanoparticles (graph 15C) but as our further results (not shown) suggested, it might be caused by the solution itself.

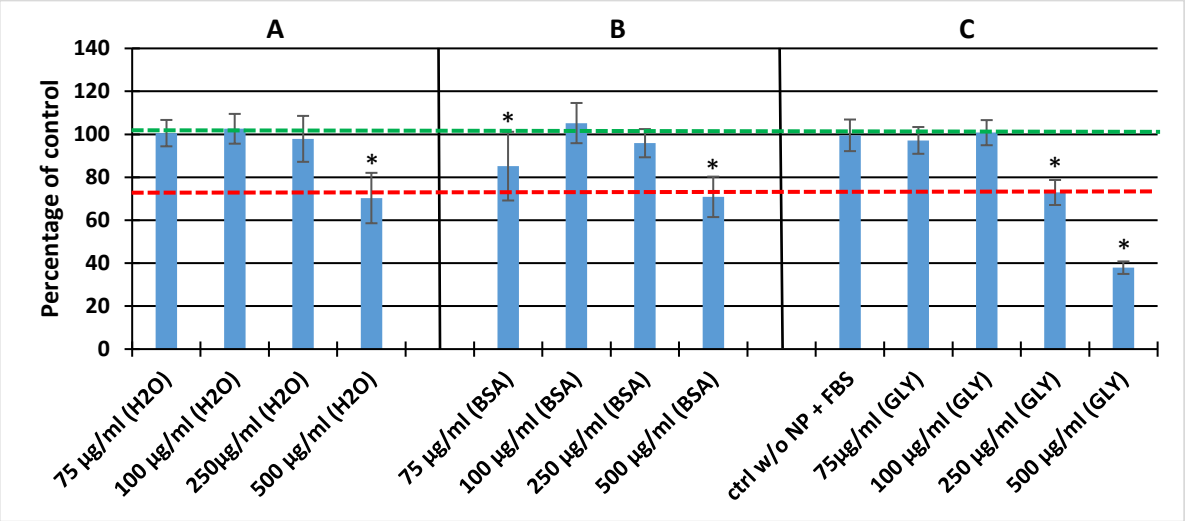

Graph 15: Metabolic activity of SAOS-2 cells measured by MTS assay after 48hours with increasing concentration of SiNPs in medium supplemented with FBS (A – SiNPs in H_2O, B – SiNPs in BSA, C – SiNPs in glycine)

Green line showing control level, red line showing cytotoxicity level of 75%

5.4. Microscopy Experiments

Since the beginning of the work, significant amount of challenges arised, for example limited amount of materials is available, conventional microscopy techniques proved to be inefficient and thus new techniques and set-ups should be introduced. Significantly more data than presented in this chapter were acquired, however, from different reasons are not representative and will not be shown. Only compact data set will be presented at the moment.

5.4.1. SiQD (Japan)

Microscopy

The above presented data from MTS and LDH tests of SiQD batch No.3 were accompanied by bright field images (fig. 9) showing morphology of the cells after 48 hours, which correlates with the obtained results from MTS assay (graph 11). Cells cultivated with SiQD in FBS-free medium revealed the same behavior and thus the data are not shown.

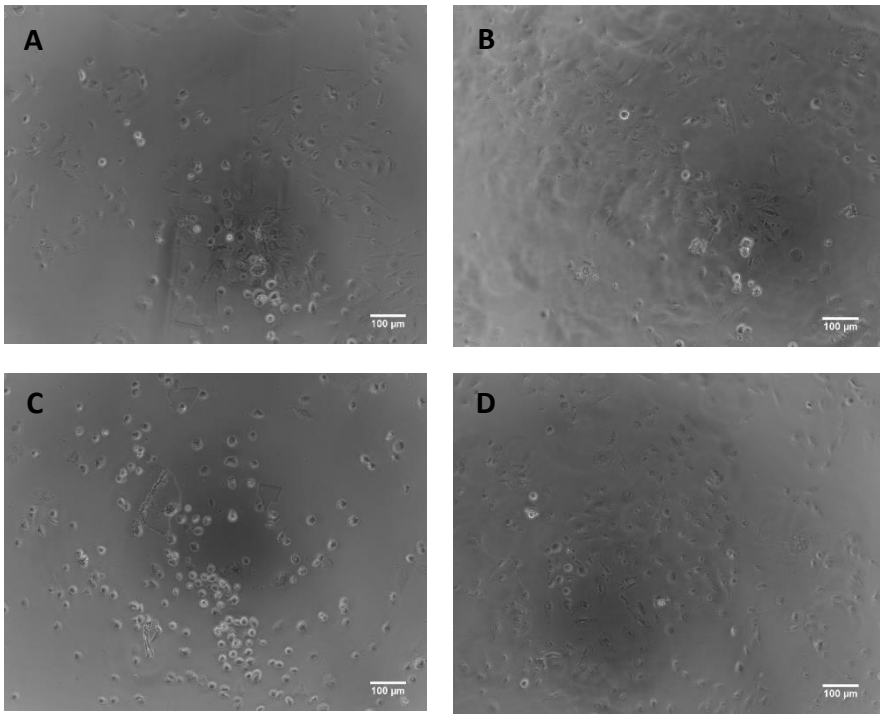

Figure 9: Bright field images of SAOS cells incubated with SiQDs for 48 h in FBS supplemented medium

A – 25 µg/ml SiQDs, B – 50 µg/ml SiQDs, C – 100 µg/ml SiQDs, D – control without SiQD treatment

Furthermore, a colocalization of SiQD with one of the structures of endocytic pathway – early endosomes (stained with EEA1 antibody), late endosomes (stained with M6PR antibody) or lysosomes (stained with LAMP2 antibody) – was conducted. This possibly simple task proved itself to be quite challenging. Even though the SiQDs possess marvelous physicochemical characteristics regarding fluorescence and its stability, in context of biological environment these advantages seemingly disappeared. Our colleagues from Faculty of Mathematics and Physics successfully proved that the particle signal was significantly quenched by the cultivation environment (Ostrovska et al., 2016). Upon

brightness and contrast enhancement in the microscope, particles can be detected after long exposure time and line accumulation, which, however, lowers the reliability of the results. Figure 10 shows results obtained after 24-hour incubation of 100 µg/ml SiQDs with SAOS-2 cells in serum - supplemented medium. Based on visual observations hardly any colocalization can be detected. However, to prove or disapprove colocalization, specialized software must be used. The quenched signal of nanoparticles however makes this quite a challenge as its enhancement by ImageJ makes the signal less reliable. So far, no nanoparticle signal can be detected within cellular nucleus region. This might point out to the premise, that nanoparticles are not present just freely in intracellular matrix, but are engulfed in some vesicle-like structures.

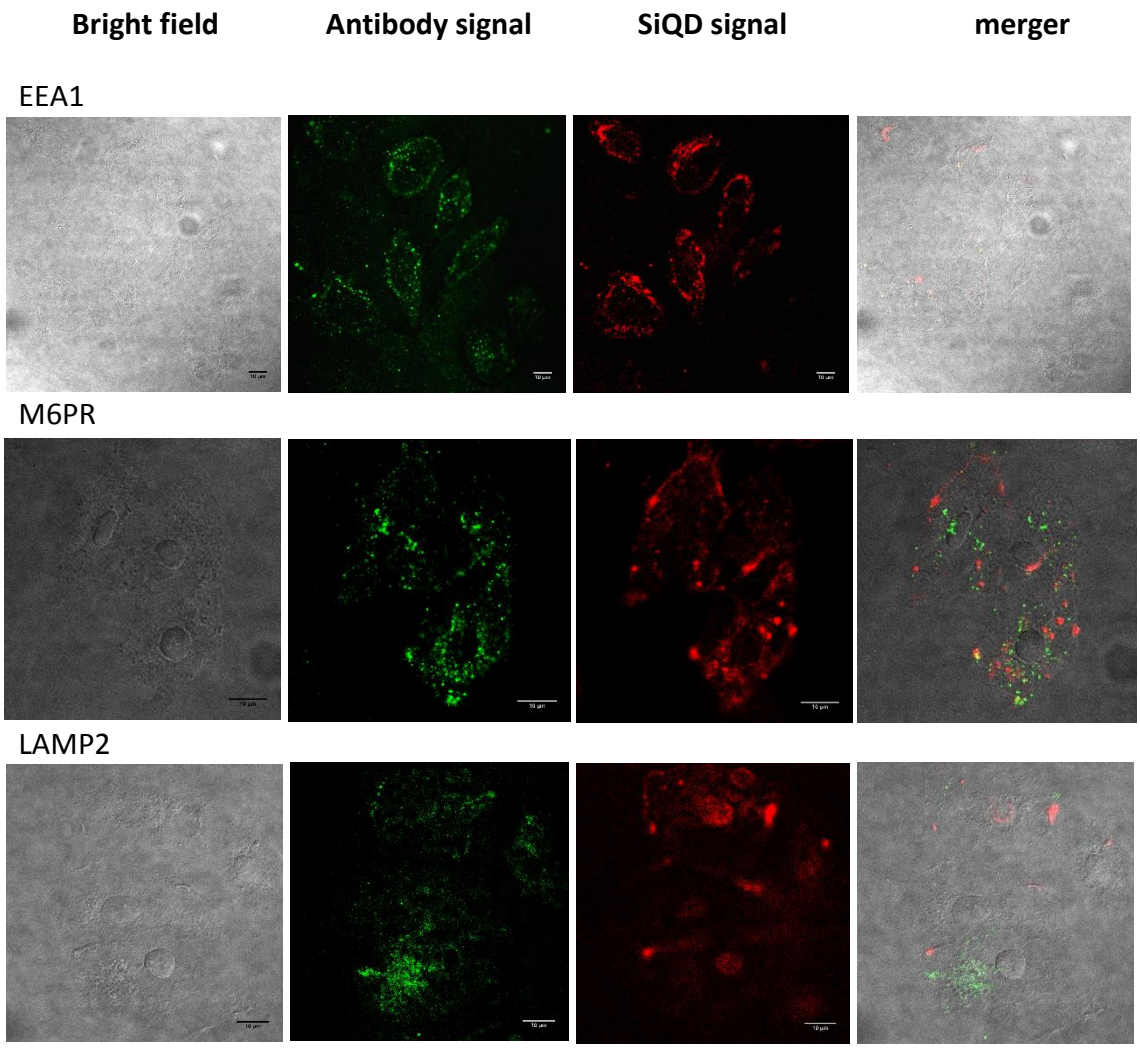

control

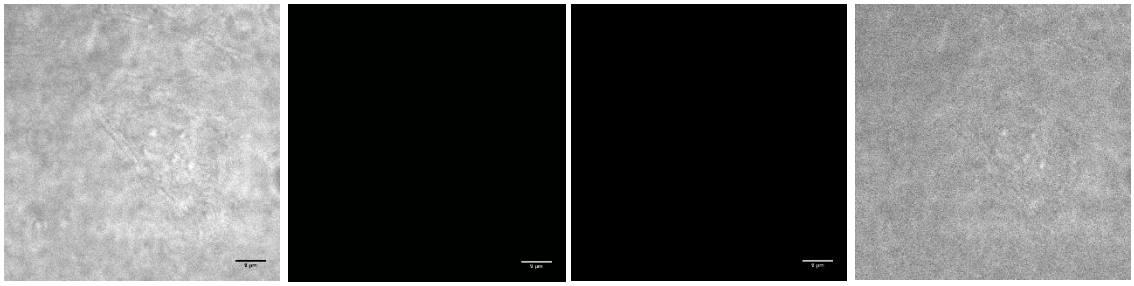

Figure 10: Microscopic observations of SAOS-2 incubated with SiQDs for 24 hours at concentration of 200 µg/ml in FBS supplemented media

Scale bar represents 10 µm

2-Photon Microscopy

As seen from the results obtained on confocal microscope, SiQDs are extremely hard to detect and thus possibility of detection by 2-photon microscopy arisen. However, as seen in fig. 11 (conducted by Josef Lazar, Ph.D), the results from 2-photon microscopy are even worse than those from confocal microscope. It turned out that 2-photon excitation in wavelengths necessary for SiQD signal acquisition also show cellular auto – fluorescence, because a signal obtained from SiQD treated cells was similar with the one obtained from control untreated cells.

Bright field **SiQD signal** **Merger**

200 µg/ml SiQD

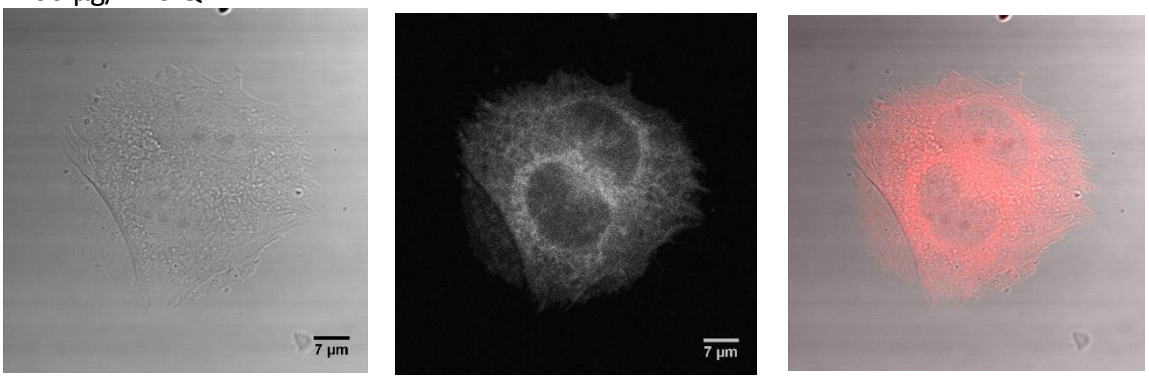

control

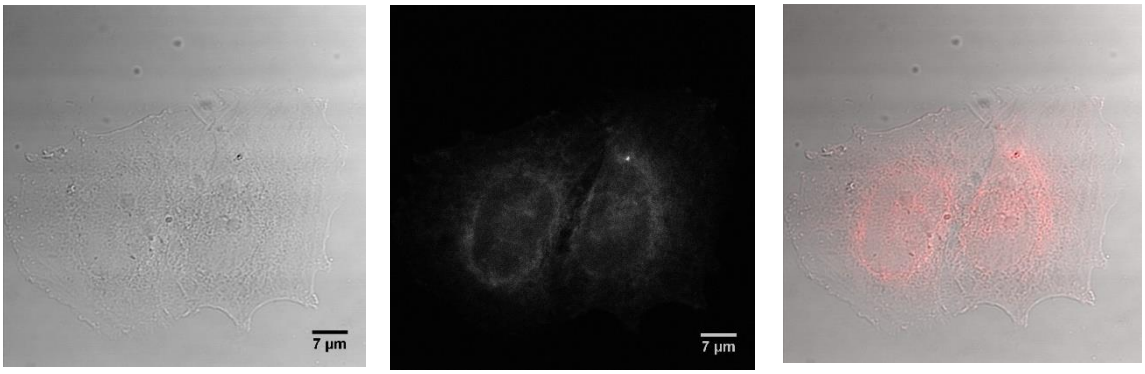

Figure 11: 2 - photon observations of SAOS-2 incubated with SiQDs for 24 hours at concentration of 200 µg/ml in serum supplemented media

Scale bar represents 7 µm

5.4.2. SiC (Hungary)

Microscopy

The SiC particles in cells were observed using Nikon Eclipse fluorescent microscope (fig. 12). For excitation UV light was used (excitation at 375 nm) and emission was acquired in DAPI channel (acquired emmision at 460 nm) at 20x magnification. This setting, however, is not ideal as debris and cellular autofluorescence may be acquired when using higher exposure times, necessary for all particle related studies. The microscopy experiments were performed using adherent THP-1 cells (THP-1 D). It was the first time this cells were used for microscopy purposes, however due to their properties they proved unusable.The THP-1 D cells are overall smaller and harder to observe than SAOS-2 cells, which is the reason why the rest of microscopy observations were performed on SAOS-2.

Bright field **SiC signal** **merger**

100 µg/ml SiCs

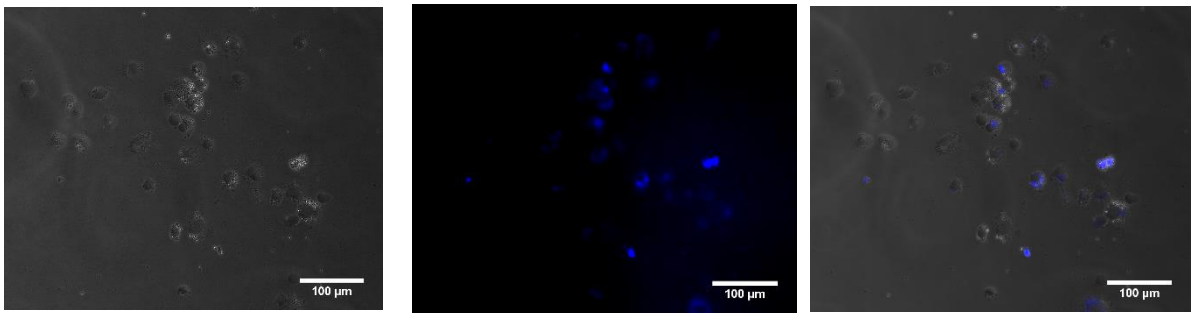

control

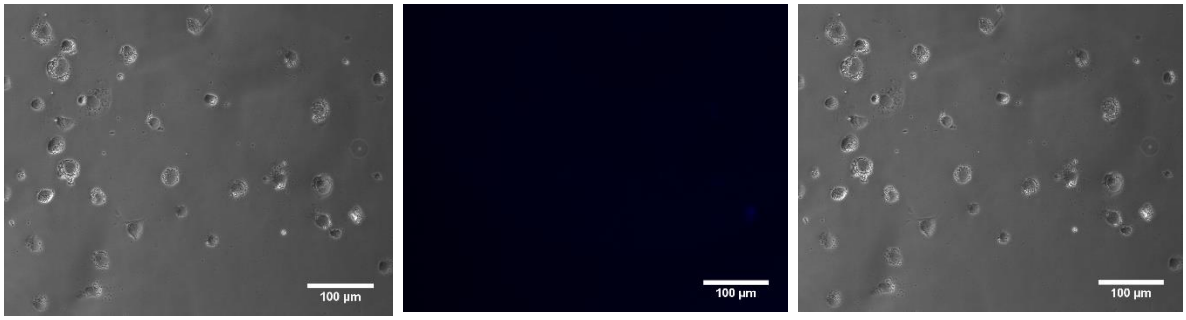

Figure 12: Microscopy observations of THP-1 D incubated with SiCs for 4 hours at concentration of 100 µg/ml in serum-supplemented media

2-Photon Microscopy

As SiC proved to interfere with auto-fluorescence signal and are hard to detect by conventional methods, 2-photon microscopy was implemented (conducted by Josef Lazar, Ph.D). Nanoparticles in concentration of 100 µg/ml were incubated with cells for 4 hours at serum-supplemented (fig. 13) and serum-free conditions (fig. 14).

Bright field **SiC signal** **Merger**

100 µg/ml SiC

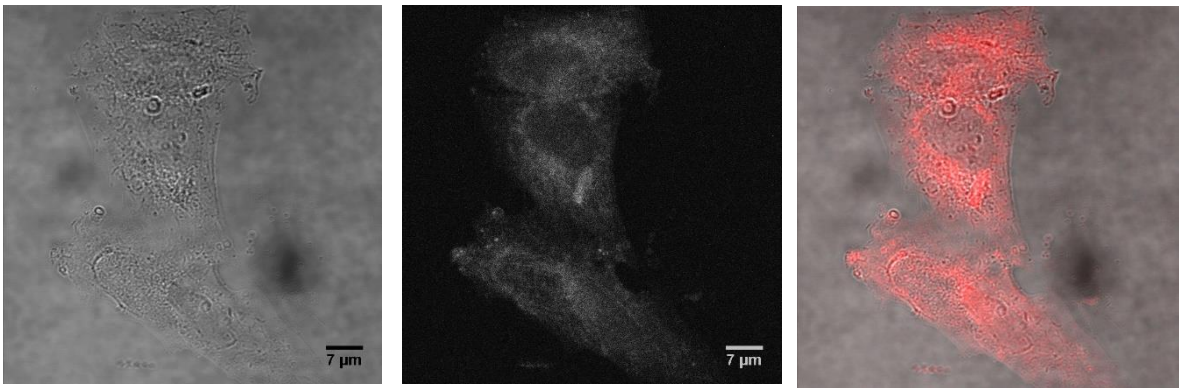

control

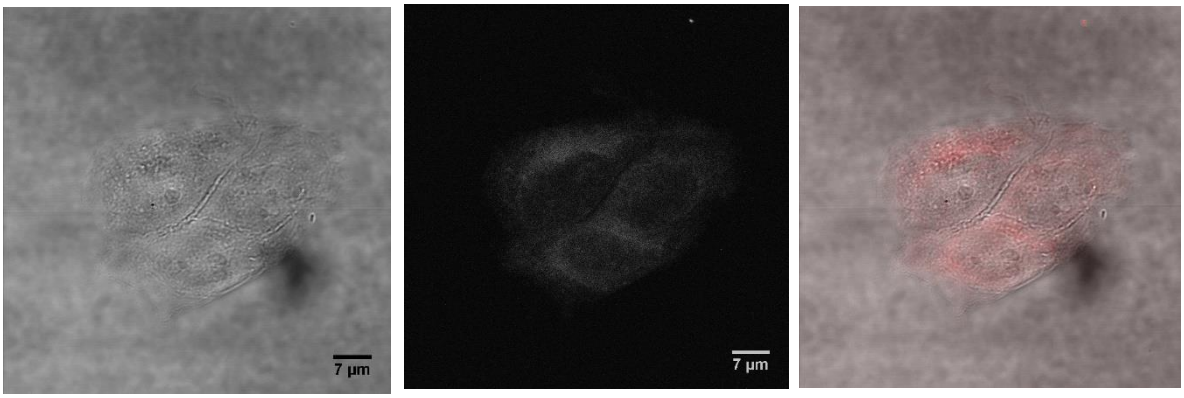

Figure 13: 2 - photon observations of SAOS-2 incubated with SiCs for 4 hours at concentration of 100 µg/ml in FBS-supplemented medium

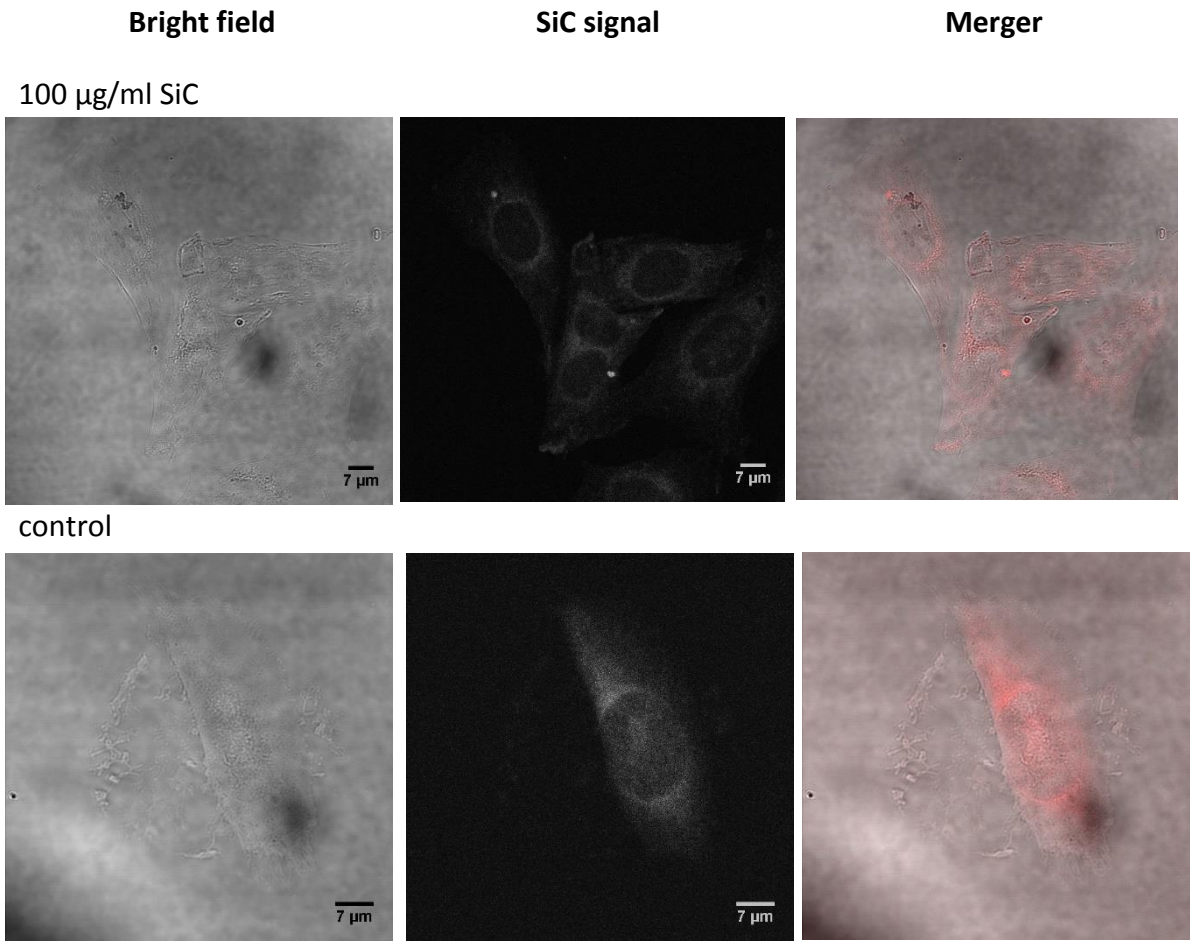

Figure 14: 2 - photon observations of SAOS-2 incubated with SiCs for 4 hours at concentration of 100 µg/ml in serum-free medium

As apparent from the above figures the particle signal is recognizable from cellular auto fluorescence (control) as it is localized in vesicle-like structures.

5.4.3. SiNP (Czech Republic)

Microscopy

As previously mentioned, these nanoparticles were provided in three different solutions (BSA, glycine and water) in order to promote their stability and alter their properties. For microscopy purposes, SAOS-2 cells were treated with 100 µg/ml of SiNPs (each solution separately) for 48 hours in FBS supplemented medium. All the images were taken using Leica confocal microscope at magnification of 63x. The impact of solution in which SiNPs were administered to cell culture showed highly important. For example, samples treated with SiNP – BSA were completely covered in debris with strong signal, which made observation

difficult. The presence of debris in SiNP – H_2O and SiNP – Gly was significantly lower and made observation of nanoparticles in cells easier. When comparing the two solutions (water and glycine) obvious difference can be spotted. The glycine treated nanoparticles can be spotted in more compact structures, whilst in water, the signal seems more diffused.

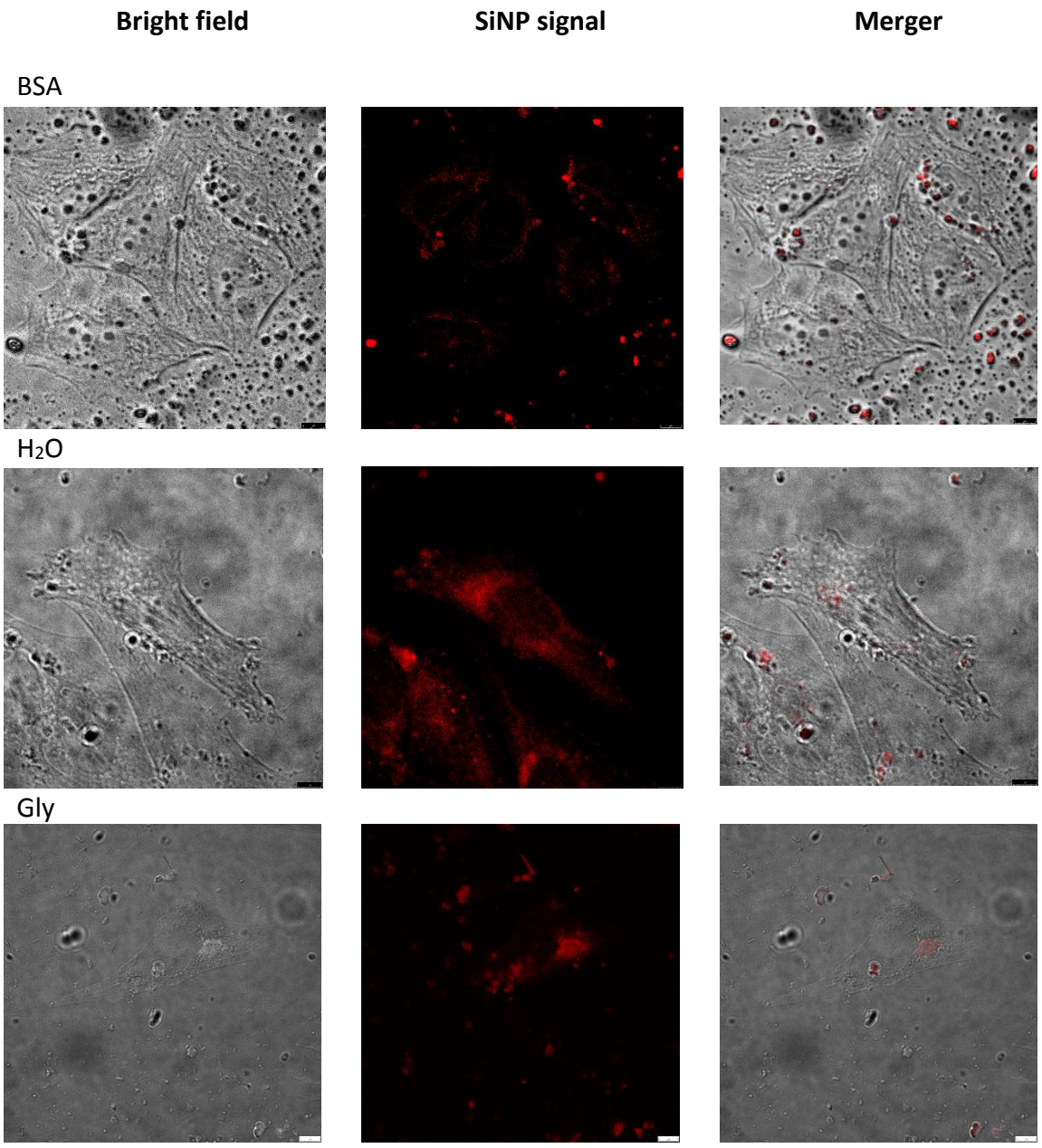

control

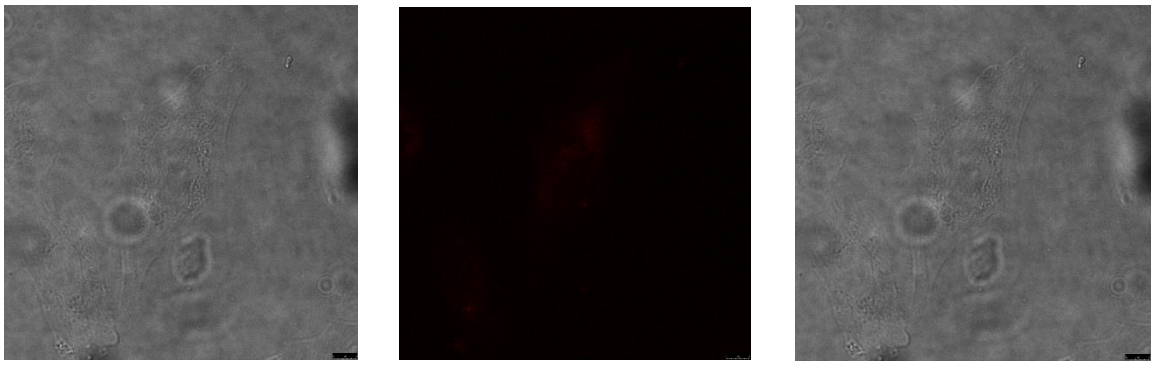

Figure 15: Microscopic observation of SAOS-2 cells incubated with SiNPs for 48 hours at concentration of 100 µg/ml in FBS-supplemented medium
Scale bar represents 8 µm

5.4.4. Transmission Electron Microscopy

Preparations of cells with golden nanoparticles for transmission electron microscopy (TEM) and necessary consultations were firstly done with doc. Ing. Pavel Ulbrich, Ph.D. (Department of Biochemistry and Microbiology, Institute of Chemical Technology in Prague). Golden nanoparticles (100 nm in diameter) from collaborating group of prof. Ing. Václav Švorčík, DrSc. (Department of Solid State Engineering, Institute of Chemical Technology in Prague) were used for the pioneer experiment, as it was more sure that these particles will be detectable by TEM. It was unclear, whether commonly used cell counts for biology experiments (metabolic activity determination, fluorescence staining and microscopy etc.) would be enough for TEM sample preparation. During the whole process the ammount used (sample including approximately 330 000 cells) showed to be insufficient due to loss of sample while handling it and no data could be acquired. As the process of preparation of TEM sample is highly time consuming and material demanding, no repetition have been done so far.

Due to time limitation at VSCHT, new contact with doc. RNDr. Dušan Cmarko, Ph.D. (Institute of Biology and Medical Genetics, First faculty of Medicine) was established and next preparations for SiQD and SiC studies were done. Firstly, we wanted to see NP alone on a TEM grid to find out if we are able to see the particles later in cells. (Fig. 16). As seen from the results, SiQDs are extremely small and hard to identify even by themselves on a bare grid. Moreover, they were provided in methanol, which we found caused destruction of TEM grid structure and made SiQD observation even harder. Unfortunately, although SiC observations were planed ahead of time, an electron microscope in the collaborating facility get under maintenance and until now has not been put back to work.

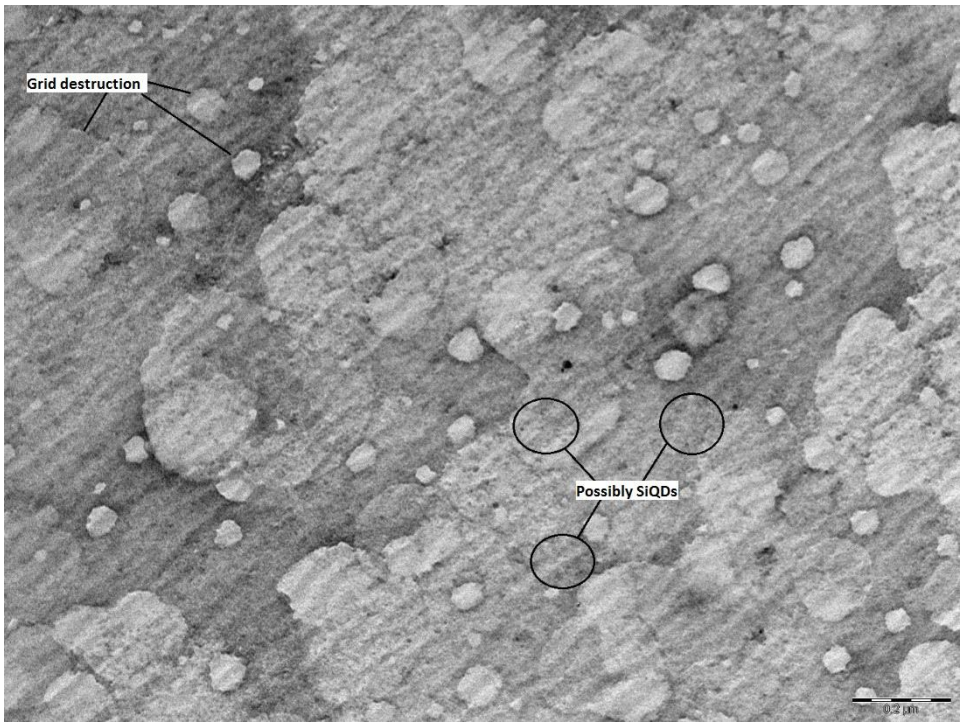

Figure 16: SiQDs in methanol on TEM grid

Circled out are possible nanoparticles hardly to be identified due to grid degradation

6. Discussion

The study is focused on the influence of different silicon-based particles on different human cells and how this influence is altered by cultivation conditions. The identification of influence mechanisms proved to be complicated, as the methods for this have not been implemented completely yet and optimization processes took longer time than expected. The presented results show cytotoxic effect of nanoparticles under different cultivation conditions, however further and deeper analysis are necessary (detection of necrosis or apoptosis). Moreover, from obtained results it is evident that conventional microscopy methods are not sufficient for deeper studies of presented nanoparticles (due to their small size of approximately 4 nm and thus relatively low quantum yield). Therefore, TEM microscopy technique is being considered and implemented for further localization studies, however it needs more time for optimization. The author intends to continue and deepen this study in her further post graduate studies on this topic, thus the results shown in this work are more of a pre-evaluations and method implementation, testing and looking for other approaches. In the following paragraphs, results from each particle type will be summarized and discussed.

6.2. Preliminary Results

At the beginning of the study, characterizations of cells and cultivation conditions establishment was done. Both cell lines used, human SAOS-2 osteoblastic cell line and human THP-1 monocytic cell line, were characterized in respect of their doubling time and basic metabolic activity. Also, in respect of THP-1 cell line, stimulation by PMA towards macrophage-like differentiation was done.

During differentiation experiments, we had to overcome the issue of not proper macrophage-like phenotype observation (fig. 4). Our laboratory had no previous experiences with this cell line and its PMA stimulated differentiation and only upon consulting with colleagues from Contipro a.s., the stumbling-block was identified to be the concentration of cells seeded for PMA stimulation. The cells probably lacked contacts with each other, which lead to incomplete transformation.

Furtherly, characterization of the PMA stimulated cells was done in order to prove whether the adherent cells are expressing macrophage markers. The flow cytometry

characterization was conducted within approximately two-month period, starting with freshly defrost cells. During this time a shift in expression profile was observed and no conclusive results were obtained (fig. 5A and B). The exact expression profiles of THP-1 derived macrophages are unclear even in literature (Aldo et al., 2014; Mittar et al., 2011).

The impact of different cultivation conditions was tested, because we are currently trying to simulate the most physiological conditions we can in *in vitro* studies. However, as seen from our results (graph 5), simulation of *in vivo* conditions by usage of HPS have significant negative impact on cellular viability. This would not be surprising due to the fact that complete HPS from an adult contains much less growth factors and more gamma globulins and complements, interfering with cells in culture. However, quite surprisingly even serum-free medium (marked in graph "simple M") showed to be more convenient for cellular metabolic activity than supplementation by either type or concentration of human sera. Interesting are also results showing slight difference between human sera from mix of donors and human sera from single donor with AB blood type. This difference may refer to the presence of antibodies in human plasma serum from donors of different blood groups, which can affect the cells. Based on our results, a compromise for physiological conditions simulation was chosen and all experiments were conducted in 5% FBS supplemented media.

6.3. SiQD (Japan)

Silicon nanoparticles co-doped with phosphorus and boron (SiQD), originating from the group of Dr. Minoru Fujii (Department of Electrical and Electronic Engineering, University of Kobe) were used for cytotoxicity studies in this thesis. These nanoparticles possess several physicochemical characteristics that make them extremely interesting. The particles have a diameter of only approximately 4 nm, possess natural fluorescence (excitation 405 nm and emission in range of 700 – 850 nm) and high quantum yield (Fujii et al.,2016).

When all the results presented in this thesis are put together, a complex image of influence of SiQDs on human cells and the role of cultivation conditions arises. All the results show similar trends but one must keep in mind, that even when particles are prepared by the same process and physicochemical properties seemingly remain the same (according to measurement of collaborating physicists), cells can identify different nanoparticle batches and react differently to them. The results from batch No.1 corresponded with our already published results, however, batch No. 2 acted completely differently and interfered with our

implemented methods (Ostrovska et al., 2016). This interference might be caused by slightly different surface characteristics or its oxidation in this batch. Batch No.3 then acted quite like the batch No.1, however, seemed to be slightly more reactive. Our colleagues from Faculty of Mathematics and Physics proposed that these changes in behavior of SiQDs might be caused by different passivation of SiQDs' surface. Passivation itself is known to change properties of nanoparticles and is time dependent (Melo et al., 2006). The time of maturation (time from fabrication until use) might have direct influence on SiQD surface properties. Thus, every new material should be tested by standardized method before using it in larger set of experiments.

Overall, the impact of SiQDs on human cells is visible and dependent on cultivation conditions. As our results suggest the presence, or more precisely the absence, of FBS as supplement in cultivation media is the key parameter influencing further impact of SiQDs on cells. Both properly functioning batches (batch No. 1 and No. 3) proved that in serum-free conditions, the impact of SiQD presence on cellular metabolic activity is significantly earlier and at lower concentrations than in FBS-supplemented media. The lack of influence on metabolic activity in FBS-supplemented medium might be caused by the formation of aggregates, which can be directly related to protein presence (Moerz et al., 2015).These aggregates do not enter cells so easily and tend to stay "stuck" to cell surface, or to cultivation surface, which might be the reason nearly no change in metabolic activity is present in FBS supplemented media.. When comparing reactions of SAOS-2 cell line and THP-1 cell line, we can assume that the more rapid and stronger reaction of THP-1 cells in FBS-free medium is caused by their natural character (phagocytic activity). It is, however, quite surprising that THP-1 cells did not reacted to nanoparticles more even in FBS - supplemented medium. Caracciolo et al. proposed that formation of biomolecular corona may have a "stealth" effect on nanoparticles, which might be the reason why the cells reacted strongly in FBS-free medium (Caracciolo et al., 2015). It would be also interesting to test their inflammatory response to nanoparticle presence in cultivation medium. This however, is only a plan for future studies.

The results regarding mechanisms of caused cytotoxicity are yet inconclusive and more repetitions must be done. However, when we compare the results from MTS assay (graph 11) with the LDH assay results (graph 12), we can assume that the mechanism is necrosis

related. LDH assay shows disruption in cellular membrane, which is directly related to necrosis. The possible activation of necrosis, however, should be discovered and studied more deeply. Presence of apoptosis was also experimentally tested, however, due to wrongly chosen assay, no results could be obtained (M30 detection assay identifies cytokeratin 18, which is not expressed by SAOS-2 nor THP-1 cells). However, for future studies, other methods for apoptosis detection, such activated caspase or annexin detection will be implemented.

Imaging and actual detection of all of the nanoparticles proved to be the most challenging task and aim. As was already proposed by Ostrovska et al. , SiQD signal is being affected and quenched by the biological environment (Ostrovska et al., 2016). This finding is quite unfortunate, as the observation of nanoparticles in cells is necessary to provide complete insight into SiQD-cell interaction. Therefore, further steps have been taken to implement TEM as possible tool for SiQD detection. However, since the beginning of the implementation, more and more challenges have arisen. This method is not only extremely time consuming, but also requires significant amounts of material (cells as well as nanoparticles). The material is probably the biggest issue, as fabrication of SiQDs takes place in Japan and is itself highly time consuming. However, despite of these inconveniences, experimental work is still in process.

6.4. SiC (Hungary)

Other particles used in this study originated from Dr. Adam Gali (Hungarian Academy of Sciences). These particles are silicon carbide composite (SiC) particles, their diameter ranges from 2 – 5 nm and they possess natural fluorescence with excitation approximately at 320 nm and emission in range of 400 – 600 nm.

These particles were tested in the same manner as previously discussed SiQDs, but showed different trends. Again, no significant reaction of SAOS-2 cells could be observed in FBS-supplemented medium, but no reaction was detected also in FBS-free medium. THP-1 cells on the other hand reacted to the presence of SiCs under both cultivation conditions. This might be caused by adherent form of THP-1 being naturally capable of phagocytosis. These particles were provided only in limited amount and so LDH assay was not conducted, which is definitely an insufficiency that must be remedied for future results. Our results could be compared to publication of the group that fabricated these nanoparticles (Beke et

al., 2013). Overall, we can confirm the results this group provided, however, we have not been as successful with microscopy as them, which might be caused by different acquisition settings, administration form (Beke et al. used direct injection into cells, whereas we have administered particles simply into cultivation medium, which might cause quenching of signal) or a little bit different nanoparticles (other batch).

6.5. SiNP (Czech Republic)

Finally, SiNPs from collaborating group of Dr. Herynková (Department of Thin Films and Nanostructures, Czech Academy of Sciences) were tested. These nanoparticles are completely different from the previously described ones. These particles are provided in the form of 100 nm clusters formed of nanocrystals with diameter of 2.5 nm and possess natural fluorescence with peak emission at about 650 nm and excitation at 405 nm (Fucikova et al., 2014). The particles were provided in three different solutions – water, glycine and BSA. Glycine and BSA were used for stabilization of physicochemical properties and prevention of further clustering.

As this cooperation started very recently, only preliminary but very promising results can be presented. The metabolic activity assay proved, that these nanoparticles are harmless even at higher concentrations than previous two types (graph 15). SAOS-2 cells in FBS-supplemented medium were only affected by the concentration of 500 μg/ml of particles after 48 hours incubation. The lowering of metabolic activity in cells treated with SiNP - glycine solution at concentration of 250 μg/ml was probably caused by the presence of glycine itself as proved by subsequent experiments, where only presence of glycine without nanoparticles was tested (data not shown). Even though these particles seem potentially harmless, MTS assay results should be accompanied by LDH assay or apoptosis detection to successfully prove it. These SiNPs also proved to be the best for imaging purposes as they were detectable more easily. Different solutions in which particles are provided, however, interfere with signal acquisition and further effort must be devoted to clearing the most debris from the samples. Their better properties for optical analysis, or more specifically the lack of signal quenching, is why these particles are possibly the only one to be tracked in live cell imaging, which is the way further research shall be oriented.

6.6. Summary

Within the past two years, a lot of challenges and difficulties have been encountered. However, the results obtained provide an interesting message. The impact of presence or absence of FBS in cultivation media while nanoparticles are administered to the cells is crucial. The mechanisms of formation and composition of biomolecular corona seems to have significant influence on nanoparticle behavior and shall be studied more deeply. Also, it is important to stress out that when speaking of nanoparticle detection in this work, clusters or vesicles containing more particles are meant, as single particle is nearly impossible to be detected.

7. Conclusions

- Determine influence of supplementation with serum on metabolic activity of human cells

After series of experiments testing different level of supplementation of cultivation media with foetal bovine serum (FBS) and human plasma serum (HPS), we have obtained several interesting results. When the cultivation medium is supplemented with FBS, the level of supplementation does not play highly important role. Cellular metabolic activity remains the same in medium supplemented with 15% FBS as well as 5% FBS. The complete absence of serum supplementation in cultivation medium significantly worsen cellular metabolic activity. Supplementation of media with human plasma serum lowered cellular metabolic activity significantly, which could be explained by low level of growth factors and other nutrition's compared to FBS. However, quite surprisingly, the metabolic activity in HPS supplemented cultivation medium was even lower than in simple medium without any serum supplements. We have also observed difference between serum from multiple unidentified donors and a donor with AB blood type. Heat treatment (inactivation) had no significant influence on the results.

- Determine influence of SiQD on viability of human cells under different cultivation conditions

The influence of SiQDs on human cells is highly dose and cultivation conditions dependent. Under FBS-free conditions, the cells show lowered metabolic activity and even some evidence of necrosis. In medium supplemented with 5% FBS, the cells are seemingly not affected. The behavior of SiQDs is, however, highly batch specific.

- Determine influence of SiC on viability of human cells under different cultivation conditions

The SiC were tested in the similar way as SiQDs but provided completely different results. The impact of these particles seems to be more dependent on cell type than on cultivation conditions. SAOS-2 cells did not react to the presence of gradually growing concentration of SiCs in cultivation media, no matter the serum supplementation. Adherent form of THP- 1 cells on the other hand reacted to nanoparticles in the same manner under both conditions.

- Determine influence of SiNP on viability of human cells

Influence of SiNPs was tested differently, as they were provided in three different solutions types. The impact of SiNPs in water, glycine and BSA solution was observed after 48 hours incubation and showed that these particles are harmful only in concentration five times higher than both previously mentioned particles. Only the solution of SiNPs in glycine showed to have impact in lower concentration, which however is more due to the glycine itself than to different particles properties.

- Use microscopy techniques to observe different types of silicon based nanoparticles in human cells

Different microscopy techniques have been used for nanoparticle observation, however proved to be insufficient and implementation of new methods was too much time demanding to accomplish. However, the SiNPs proved to be the most promising platform for further microscopy observations as their signal is not quenched by the cultivation medium, which happens in SiQDs as well as in SiCs. Further colocalization studies and 3D and live cell imaging are necessary to prove the presence of nanoparticles inside of the cells as well as the actual uptake mechanism.

8. References

Aldo, P. B., Craveiro, V., Guller, S., & Mor, G. (2014). Effect of culture conditions on the phenotype of THP-1 monocyte cell line, *70*(1), 80–86. https://doi.org/10.1111/aji.12129.Effect

Anglin, E. J., Schwartz, M. P., Ng, V. P., Perelman, L. a., & Sailor, M. J. (2004). Engineering the chemistry and nanostructure of porous silicon Fabry-Pérot Films for Loading and Release of a Steroid. *Langmuir*, *20*(25), 11264–11269. https://doi.org/10.1021/la048105t

Athinarayanan, J., Periasamy, V. S., Alhazmi, M., Alatiah, K. a, & Alshatwi, A. a. (2015). Synthesis of biogenic silica nanoparticles from rice husks for biomedical applications. *Ceramics International*, *41*(1), 275–281. https://doi.org/10.1016/j.ceramint.2014.08.069

Beke, D., Szekrényes, Z., Pálfi, D., Róna, G., Balogh, I., Maák, P. A., … Gali, A. (2013). Silicon carbide quantum dots for bioimaging. *Journal of Materials Research*, *28*(2), 205–209. https://doi.org/10.1557/jmr.2012.296

Brown, D. M., Kanase, N., Gaiser, B., Johnston, H., & Stone, V. (2014). Inflammation and gene expression in the rat lung after instillation of silica nanoparticles : Effect of size , dispersion medium and particle surface charge. *Toxicology Letters*, *224*(1), 147–156. https://doi.org/10.1016/j.toxlet.2013.10.019

Burdette, M. K., Jenkins, R., Bandera, Y., Powell, R. R., Bruce, T. F., Yang, X., … Foulger, S. H. (2016). Bovine serum albumin coated nanoparticles for in vitro activated fluorescence. *Nanoscale*, *8*(48), 20066–20073. https://doi.org/10.1039/C6NR05883C

Caracciolo, G., Palchetti, S., Colapicchioni, V., Digiacomo, L., Pozzi, D., Capriotti, A. L., … Lagan, A. (2015). Stealth Effect of Biomolecular Corona on Nanoparticle Uptake by Immune Cells. *Langmuir*, *31*(39), 10764–10773. https://doi.org/10.1021/acs.langmuir.5b02158

Casals, E., & Puntes, V. F. (2012). Inorganic nanoparticle biomolecular corona: formation, evolution and biological impact. *Nanomedicine (London, England)*, *7*(12), 1917–30. https://doi.org/10.2217/nnm.12.169

Drbohlavova, J., Adam, V., Kizek, R., & Hubalek, J. (2009). Quantum dots - characterization, preparation and usage in biological systems. *International Journal of Molecular Sciences*, *10*(2), 656–673. https://doi.org/10.3390/ijms10020656

Elsaesser, A., & Howard, C. V. (2012). Toxicology of nanoparticles. *Advanced Drug Delivery Reviews*, *64*(2), 129–137. https://doi.org/10.1016/j.addr.2011.09.001

Flahaut, E., Durrieu, M. C., Remy-Zolghadri, M., Bareille, R., & Baquey, C. (2006). Investigation of the cytotoxicity of CCVD carbon nanotubes towards human umbilical vein endothelial cells. *Carbon*, *44*(6), 1093–1099. https://doi.org/10.1016/j.carbon.2005.11.007

Fröhlich, E. (2012). The role of surface charge in cellular uptake and cytotoxicity of medical nanoparticles. *International Journal of Nanomedicine*, *7*, 5577–5591. https://doi.org/10.2147/IJN.S36111

Fucikova, A., Valenta, J., Pelant, I., Kalbacova, M. H., Broz, A., Rezek, B., … Bakaeva, Z. (2014).

Silicon nanocrystals and nanodiamonds in live cells: photoluminescence characteristics, cytotoxicity and interaction with cell cytoskeleton. *RSC Advances*, *4*, 10334. https://doi.org/10.1039/c3ra47574c

Fujii, M., Sugimoto, H., & Imakita, K. (2016). All-inorganic colloidal silicon nanocrystals — surface modi fi cation by boron and phosphorus co-doping. *Nanotechnology*, *27*(26).

Gagner, J. E., Qian, X., Lopez, M. M., Dordick, J. S., & Siegel, R. W. (2012). Effect of gold nanoparticle structure on the conformation and function of adsorbed proteins. *Biomaterials*, *33*(33), 8503–8516. https://doi.org/10.1016/j.biomaterials.2012.07.009

Gratton, S. E. a, Ropp, P. a, Pohlhaus, P. D., Luft, J. C., Madden, V. J., Napier, M. E., & DeSimone, J. M. (2008). The effect of particle design on cellular internalization pathways. *Proceedings of the National Academy of Sciences of the United States of America*, *105*(33), 11613–11618. https://doi.org/10.1073/pnas.0801763105

Guo, C., Xia, Y., Niu, P., Jiang, L., Duan, J., Yu, Y., … Sun, Z. (2015). Silica nanoparticles induce oxidative stress, inflammation, and endothelial dysfunction in vitro via activation of the MAPK/Nrf2 pathway and nuclear factor-κB signaling. *International Journal of Nanomedicine*, *10*, 1463–1477. https://doi.org/10.2147/IJN.S76114

Halas, N. J. (2008). Nanoscience under glass: The versatile chemistry of silica nanostructures. *ACS Nano*, *2*(2), 179–183. https://doi.org/10.1021/nn800052e

Han, X., Lai, L., Tian, F., Jiang, F.-L., Xiao, Q., Li, Y., … Liu, Y. (2012). Toxicity of CdTe Quantum Dots on Yeast Saccharomyces Cerevisiae. *Small*, *8*(17), 2680–2689. https://doi.org/10.1002/smll.201200591

Herd, H., Daum, N., Jones, A. T., Huwer, H., Ghandehari, H., Lehr, C., … Technology, P. (2013). Nanoparticle Geometry and Surface Orientation In fl uence Mode of Cellular Uptake, (Xx), 1961–1973.

Chu, Z., Huang, Y., Li, L., Tao, Q., & Li, Q. (2012). Physiological pathway of human cell damage induced by genotoxic crystalline silica nanoparticles. *Biomaterials*, *33*(30), 7540–7546. https://doi.org/10.1016/j.biomaterials.2012.06.073

Jiang, W., Kim, B. Y. S., Rutka, J. T., & Chan, W. C. W. (2008). Nanoparticle-mediated cellular response is size-dependent. *Nature Nanotechnology*, *3*(3), 145–150. https://doi.org/10.1038/nnano.2008.30

Kasper, J., Hermanns, M. I., Bantz, C., Utech, S., Koshkina, O., Maskos, M., … James Kirkpatrick, C. (2013). Flotillin-involved uptake of silica nanoparticles and responses of an alveolar-capillary barrier in vitro. *European Journal of Pharmaceutics and Biopharmaceutics*, *84*(2), 275–287. https://doi.org/10.1016/j.ejpb.2012.10.011

Kim, I. Y., Joachim, E., Choi, H., & Kim, K. (2015). Toxicity of silica nanoparticles depends on size, dose, and cell type. *Nanomedicine: Nanotechnology, Biology, and Medicine*, *11*(6), 1407–1416. https://doi.org/10.1016/j.nano.2015.03.004

Kuhn, D. A., Vanhecke, D., Michen, B., Blank, F., Gehr, P., Petri-fink, A., & Rothen-rutishauser, B. (2014). Different endocytotic uptake mechanisms for nanoparticles in epithelial cells and macrophages, 1625–1636. https://doi.org/10.3762/bjnano.5.174

Lauerová, L., Kovarik, J., Bártek, J., Rejthar, A., & Vojtěsek, B. (1988). Novel Monoclonal Antibodies Defining Epitope of Human Cytokeratin 18 Molecule. *Hybridoma*, *7*(5), 495–504.

Lehman, S. E., Morris, A. S., Mueller, P. S., Salem, A. K., Grassian, V. H., & Larsen, S. C. (2016). Silica nanoparticle-generated ROS as a predictor of cellular toxicity: mechanistic insights and safety by design. *Environ. Sci.: Nano*, *3*(1), 56–66. https://doi.org/10.1039/C5EN00179J

Lesniak, A., Fenaroli, F., Monopoli, M. P., Åberg, C., Dawson, K. a., & Salvati, A. (2012). Effects of the presence or absence of a protein corona on silica nanoparticle uptake and impact on cells. *ACS Nano*, *6*(7), 5845–5857. https://doi.org/10.1021/nn300223w

Li, L., Liu, T., Fu, C., Tan, L., Meng, X., & Liu, H. (2015). Biodistribution , excretion , and toxicity of mesoporous silica nanoparticles after oral administration depend on their shape. *Nanomedicine: Nanotechnology, Biology, and Medicine*, *11*(8), 1915–1924. https://doi.org/10.1016/j.nano.2015.07.004

Melo, T. F. O., da Silva, S. W., Soler, M. a. G., Lima, E. C. D., & Morais, P. C. (2006). Investigation of surface passivation process on magnetic nanoparticles by Raman spectroscopy. *Surface Science*, *600*(18), 3642–3645. https://doi.org/10.1016/j.susc.2006.02.055

Mirshafiee, V., Kim, R., Park, S., Mahmoudi, M., & Kraft, M. L. (2016). Impact of protein pre-coating on the protein corona composition and nanoparticle cellular uptake. *Biomaterials*, *75*, 295–304. https://doi.org/10.1016/j.biomaterials.2015.10.019

Mittar, D., Paramban, R., & Mcintyre, C. (2011). Flow Cytometry and High-Content Imaging to Identify Markers of Monocyte-Macrophage Differentiation. *BD Biosciences*, (August), 20. https://doi.org/papers3://publication/uuid/05466CA5-7EF6-409B-8CA3-30840B508BB3

Moerz, S. T., Kraegeloh, A., Chanana, M., & Kraus, T. (2015). Formation Mechanism for Stable Hybrid Clusters of Proteins and Nanoparticles, (7), 6696–6705.

Monopoli, M. P., Aberg, C., Salvati, A., & Dawson, K. A. (2012). Biomolecular coronas provide the biological identity of nanosized materials. *Nat Nano*, *7*(12), 779–786. Retrieved from http://dx.doi.org/10.1038/nnano.2012.207

Napierska, D., Thomassen, L. C. J., Rabolli, V., Lison, D., Gonzalez, L., Kirsch-volders, M., … Hoet, P. H. (2009). Size-Dependent Cytotoxicity of Monodisperse Silica Nanoparticles in Human Endothelial Cells, (7), 846–853. https://doi.org/10.1002/smll.200800461

Nowak, J. S., Mehn, D., Nativo, P., García, C. P., Gioria, S., Ojea-jiménez, I., & Gilliland, D. (2014). Silica nanoparticle uptake induces survival mechanism in A549 cells by the activation of autophagy but not apoptosis, *224*, 84–92. https://doi.org/10.1016/j.toxlet.2013.10.003

Oh, N., & Park, J.-H. (2014). Endocytosis and exocytosis of nanoparticles in mammalian cells. *International Journal of Nanomedicine*, *9*, 51–63. https://doi.org/10.2147/IJN.S26592

Ostrovska, L., Broz, A., Fucikova, A., Belinova, T., Sugimoto, H., Kanno, T., … Kalbacova, M. H. (2016). The impact of doped silicon quantum dots on human osteoblasts. *RSC Adv.*, *6*, 63403–63413. https://doi.org/10.1039/C6RA14430F

Peng, F., Su, Y., Zhong, Y., Fan, C., Lee, S. T., & He, Y. (2014). Silicon nanomaterials platform for bioimaging, biosensing, and cancer therapy. *Accounts of Chemical Research*, *47*(2), 612–623. https://doi.org/10.1021/ar400221g

Perevedentseva, E., Hong, S. F., Huang, K. J., Chiang, I. T., Lee, C. Y., Tseng, Y. T., & Cheng, C.

L. (2013). Nanodiamond internalization in cells and the cell uptake mechanism. *Journal of Nanoparticle Research*, *15*. https://doi.org/10.1007/s11051-013-1834-8

Rejman, J., Oberle, V., Zuhorn, I. S., & Hoekstra, D. (2004). Size-dependent internalization of particles via the pathways of clathrin- and caveolae-mediated endocytosis. *The Biochemical Journal*, *377*(Pt 1), 159–169. https://doi.org/10.1042/BJ20031253

Salvati, A., Pitek, A. S., Monopoli, M. P., Prapainop, K., Bombelli, F. B., Hristov, D. R., … Dawson, K. a. (2013). Transferrin-functionalized nanoparticles lose their targeting capabilities when a biomolecule corona adsorbs on the surface. *Nature Nanotechnology*, *8*(2), 137–43. https://doi.org/10.1038/nnano.2012.237

Shao, L., Gao, Y., & Yan, F. (2011). Semiconductor Quantum Dots for Biomedicial Applications, 11736–11751. https://doi.org/10.3390/s111211736

Slowing, I. I., Vivero-escoto, J. L., Zhao, Y., Kandel, K., Peeraphatdit, C., Trewyn, B. G., & Lin, V. S. Y. (2011). Exocytosis of mesoporous silica nanoparticles from mammalian cells : from asymmetric cell-to-cell transfer to protein harvesting. *Small*, *7*(11). https://doi.org/10.1002/smll.201002077

Slowing, I., Trewyn, B. G., & Lin, V. S.-Y. (2006). Effect of surface functionalization of MCM-41-type mesoporous silica nanoparticles on the endocytosis by human cancer cells. *Journal of the American Chemical Society*, *128*(46), 14792–14793. https://doi.org/10.1021/ja0645943

Stayton, I., Winiarz, J., Shannon, K., & Ma, Y. (2009). Study of uptake and loss of silica nanoparticles in living human lung epithelial cells at single cell level. *Analytical and Bioanalytical Chemistry*, *394*(6), 1595–1608. https://doi.org/10.1007/s00216-009-2839-0

Tamba, B. I., Dondas, a., Leon, M., Neagu, a. N., Dodi, G., Stefanescu, C., & Tijani, a. (2015). Silica nanoparticles: Preparation, characterization and in vitro/in vivo biodistribution studies. *European Journal of Pharmaceutical Sciences*, (February). https://doi.org/10.1016/j.ejps.2015.02.002

Tenzer, S., Docter, D., Kuharev, J., Musyanovych, A., Fetz, V., Hecht, R., … Stauber, R. H. (2013). Rapid formation of plasma protein corona critically affects nanoparticle pathophysiology. *Nature Nanotechnology*, *8*(September), 772–81. https://doi.org/10.1038/nnano.2013.181

Treuel, L., Brandholt, S., Maffre, P., Wiegele, S., Shang, L., & Nienhaus, U. (2014). Impact of Protein Modi fi cation on the Protein Corona on Nanoparticles and Nanoparticle À Cell Interactions, (1), 503–513.

Trewyn, B. G., Nieweg, J. a., Zhao, Y., & Lin, V. S.-Y. (2008). Biocompatible mesoporous silica nanoparticles with different morphologies for animal cell membrane penetration. *Chemical Engineering Journal*, *137*(1), 23–29. https://doi.org/10.1016/j.cej.2007.09.045

Wu, Y., Tang, W., Wang, P., Liu, C., Yuan, Y., & Qian, J. (2015). Cytotoxicity and Cellular Uptake of Amorphous Silica Nanoparticles in Human Cancer Cells, 779–787. https://doi.org/10.1002/ppsc.201400167

Yanes, R. E., Tarn, D., Hwang, A. A., Ferris, D. P., Sherman, S. P., Thomas, C. R., … Zink, J. I. (2013). Involvement of Lysosomal Exocytosis in the Excretion of Mesoporous Silica

Nanoparticles and Enhancement of the Drug Delivery Effect by Exocytosis Inhibition, 697–705. https://doi.org/10.1002/smll.201201811

Zhang, S., Chu, Z., Yin, C., Zhang, C., Lin, G., & Li, Q. (2013). Controllable Drug Release and Simultaneously Carrier Decomposition of SiO 2 ‐Drug Composite Nanoparticles. *Journal of American Chemical Society*, *135*, 5709–5716.

Zheng, H., Chen, G., Song, F., DeLouise, L. A., & Lou, Z. (2011). The cytotoxicity of OPA-modified Cdse/Zns core/shell quantum dots and its modulation by silibinin in human skin cells. *Journal of Biomedical Nanotechnology*, *7*(5), 648–658. https://doi.org/10.1166/jbn.2011.1331

Online references:

The Cell: A Molecular Approach. 2nd edition:2000(en). [cited 2017-08-07].Bookshelf ID: NBK9831. Avaliable at: https://www.ncbi.nlm.nih.gov/books/NBK9831/

"ISO/TS 27687:2008(en)." [cited 2017-08-07]. 2012, Nanotechnologies: Terminology and definitions for nano-objects: Nanoparticle, nanofibre and nanoplate. London: British Standards Institution. Avaliable at: https://www.iso.org/obp/ui/#iso:std:iso:ts:27687:ed-1:v2:en